Evolutionary invasion analysis for structured populations: a synthesis

Ryosuke Iritani[1] and Troy Day[2]

[1]RIKEN Center for Interdisciplinary Theoretical and Mathematical Sciences, Saitama, Japan
[2]Department of Mathematics and Statistics, Queen's University, Canada

March 24, 2026

Abstract

Natural populations exhibit complex class structures that profoundly shape evolutionary trajectories. While evolutionary demography provides a formal framework to predict adaptation using invasion fitness, the high mathematical dimensionality of these models often precludes analytical solutions, obscuring biological interpretation and hindering the analysis of long-term evolutionary outcomes. Because current reduction techniques remain fragmented, a unifying theoretical foundation is critically needed. Here, we introduce "structural evolutionary invasion analysis," a systematic framework that integrates two complementary tools to simplify complex life cycles. First, we formulate the "invasion determinant," an algebraic method that yields a direct scalar condition for mutant invasion. Second, we develop the Projected Next-Generation Matrix (PNGM), which structurally compresses life-cycle graphs by eliminating secondary classes. We demonstrate that this reduction is mathematically equivalent to separating dynamical timescales, explicitly preserving Fisher's reproductive values for the retained focal classes. Crucially, under the standard assumption of weak selection, our synthesized framework guarantees that all properties of evolutionary singularities—including their location, convergence stability, and evolutionary stability—are strictly identical to those derived from the full, unreduced model. Illustrated with diverse ecological examples, this framework provides modellers with a rigorous and tractable toolkit for decoding state-dependent selection in high-dimensional populations.

1 Introduction

Natural populations exhibit complex structures, defined by state variables such as sex, age, body size, or habitat quality. This class structure profoundly shapes individual life histories, generating substantial heterogeneity in the selection pressures experienced across different classes. Theoretical studies have revealed that such state-dependent selection is the primary driver behind a vast array of evolutionary phenomena, from conditional sex allocation and differential dispersal to facultative social behaviours and pathogen defences (e.g., Rodrigues & Gardner 2013; Rodrigues & Gardner 2015; Úbeda & Jansen 2016; Iritani & Cheptou 2017; Boots & Best 2018; Iritani et al. 2019; Kuijper & Johnstone 2019; Buckingham et al. 2023). Crucially, empirical research has increasingly corroborated these theoretical predictions, explicitly quantifying how selection gradients and life-history trade-offs vary dynamically across ages, physical conditions, or environmental patches in wild populations (e.g., Coulson et al. 2005; Pelletier et al. 2007; Kruuk & Hill 2008). For example, specific trade-off structures have been shown to drive the evolution of antagonistic pleiotropy, with differential selection operating across distinct life-history stages (Guillaume & Otto 2012). Therefore, elucidating how class structure modulates natural selection is not merely a descriptive task, but a fundamental prerequisite for predicting evolutionary trajectories in realistic biological systems.

To mathematically capture this complex state-dependent selection, evolutionary dynamics in class-structured populations are predominantly analyzed through "evolutionary demography", a powerful synthesis of adaptive dynamics (evolutionary invasion analysis) and matrix population models (Metz et al. 1992; Takada & Nakajima 1992; Dieckmann & Law 1996; Geritz et al. 1998; Caswell 2001; Rees & Ellner 2016). This analytical framework translates the demographic transitions of individuals across different classes into the invasion fitness (i.e., the asymptotic growth rate) of a rare mutant lineage. Crucially, successful invasion in structured populations depends not simply on immediate offspring production, but on the long-term, relative demographic contribution of each state, rigorously quantified as class-specific reproductive values (Fisher 1930; Taylor 1990;

Caswell 2001; Rousset 2004). By explicitly linking demographic mechanics to these reproductive values, the evolutionary demography framework provides the essential theoretical machinery to decode how adaptive evolution proceeds amidst inherent population heterogeneity.

One technical challenge is to obtain an analytically tractable expression for the invasion growth rate. This calculation typically involves determining the eigenvalues of a Jacobian matrix, which describes the short-term growth of the mutant population. Yet, eigenvalues often lack closed-form expressions, and even when they are obtainable, their biological interpretation is frequently obscure. To address this challenge, Hurford et al. (2010) developed the next-generation matrix approach building on earlier advances in mathematical epidemiology (Diekmann et al. 1990; van den Driessche & Watmough 2002). The core idea is to transform the Jacobian into an alternative matrix (the 'next-generation matrix') that captures the lifetime reproductive output of individuals in each class. This next-generation matrix allows us to calculate the expected number of offspring produced over an individual's lifetime and enables a systematic characterization of invasion conditions in the form of $R_0 > 1$, where unity represents the threshold value for reproductive success. Because the invasion condition determines the long-term consequence of evolution, evaluating the form of R_0 can yield crucial biological insights.

Nevertheless, the next-generation approach faces its own limitations, particularly in systems with higher dimensionality. Even in relatively simple cases, the biological interpretation of the invasion condition remains obscure. For example, Massol & Débarre (2015) analyzed the next-generation matrix of evolutionary dynamics of dispersal in a metapopulation composed of two habitat types (good and poor quality). They derived the invasion condition as a solution to a quadratic equation, yet the biological interpretation of the solution remained obscure. Such problems become more pronounced in systems with greater dimensionality, where obtaining simple or interpretable invasion conditions is generally elusive.

The mathematical dimensionality of these models scales directly with the number of population classes. Several studies have proposed methods to reduce the dimension of class-structured population models, although primarily in ecological or epidemiological contexts rather than evolutionary settings (Caswell 2001; de Camino Beck & Lewis 2007; Rueffler & Metz 2013; Lewis et al. 2019). Rueffler et al. (2012) applied a linear algebraic approach to life-history evolution, illustrating the relevance of the optimization principle (Charnov 1976). However, their work did not offer a systematic way to derive biologically interpretable invasion conditions. Similarly, Roberts & Heesterbeek (2003) proposed the type-reproduction number approach, which allows for focusing on the spread of disease in a subset of compartments (classes) in the host population and thereby reducing the model dimension. However, despite its general utility, its application to evolutionary invasion analysis remains scarce.

In this article, we formulate a unifying framework, which we term structural evolutionary invasion analysis, for deriving the invasion condition of a mutant in class-structured populations. We present two complementary methods—the invasion determinant and the Projected Next-Generation Matrix (PNGM)—that are applicable to any class-structured model. We highlight the pros and cons of these methods in the context of Fisher's theory of reproductive value (Fisher 1930; Taylor 1990; Caswell 2001; Rousset 2004). Following Caswell (2001) and Rueffler et al. (2012), we also use life-cycle graphs to highlight the biological interpretation of these methods. Notably, these proposed methods can be seamlessly combined. We illustrate their utility by applying them to four examples drawn from the literature. Although we assume weak selection (i.e., the phenotypic effect of mutation is small) throughout the manuscript, this synthesized framework provides modellers with powerful tools to simplify complex analyses and derive meaningful biological predictions.

2 Overview: Evolutionary invasion analysis

We first review the next-generation matrix (NGM) methodology for evolutionary invasion analysis within the adaptive dynamics framework (Hofbauer & Sigmund 1990; Dieckmann & Law 1996; Geritz et al. 1998; Hurford et al. 2010). In general, we begin by modelling nonlinear ecological dynamics of a class-structured, monomorphic population. Models may be cast in continuous time (ordinary differential equations) or discrete time (recursions). For now, we focus on the continuous-time dynamics and examine the discrete-time case later in the Examples section. The generic notation is summarized in Table 1.

Table 1: Summary of notation used in the main text.

Notation	Definition	Note
K	number of classes	
k, m	class labels	$\in \{1, 2, \dots, K\}$
$\in$	membership	
z	evolving trait	z for resident; z' for mutant
$'$	mutant (superscript)	
$\circ$	resident/neutrality (superscript)	
δ	phenotypic effect of mutation	$= z' - z$; assumed small
N_k	density in class k	N_k for resident; N_k for mutants
$\top$	transpose	
$\vec{N}$	vector of densities	$= (N_1, \dots, N_K)^\top$
A	rate of change in densities	matrix with elements $a_{k,m}$
^{C} or ^{D}	continuous-time or discrete-time	used for Jacobian label
J	Jacobian of mutant dynamics	J^{D} for discrete-time model
σ	largest real part of the eigenvalues	spectral abscissa
U	inflow rate matrix (typically birth)	subcomponent of J
V	remaining terms in J	$U - V = J$
F	birth matrix	need not be 'birth'
S	state-transition matrix	need not be 'transition'
G	next-generation matrix (NGM)	defined as UV^{-1} (or similar)
$g_{k,m}$	(k, m)-element of G	gene transfer to class k from class m
R_0	reproduction number (generic)	$\rho(G)$; $R_0 > 1$ implies invasion
ρ	largest absolute value of the eigenvalues	spectral radius
$\mathbb{X}$	primary group of classes	
$\mathbb{Y}$	secondary group of classes	$\mathbb{X} \cup \mathbb{Y} = \{1, 2, \dots, K\}, \mathbb{X} \cap \mathbb{Y} = \varnothing$
$\vec{N_{\mathbb{X}}}, \vec{N_{\mathbb{Y}}}$	density vector of primary/secondary group	
$\mathcal{R}_{\mathbb{X}}(G)$	Projected NGM (PNGM)	NGM projected onto $\mathbb{X}$

We follow a standard adaptive dynamics approach and assume that the rate of mutation is small enough that the ecological dynamics reach an equilibrium while monomorphic (referred to as resident equilibrium). Biologically, we separate the timescales of ecological and evolutionary dynamics. We also assume that the effect of mutations is small, meaning that the strength of natural selection is weak. Specifically, we suppose the resident equilibrium is monomorphic with trait value z; this trait is assumed to be a quantitative trait, possibly multidimensional. We then consider a slightly different mutant phenotype $z' = z + \delta$, where δ is the small phenotypic effect of mutation.

We primarily focus on evaluating the invasion condition. This focus is grounded in the "invasion implies substitution" principle (Geritz 2005; Priklopil & Lehmann 2020): under the assumption of rare mutations, a mutant that satisfies the invasion condition is expected to fix in the population, driving the system to a new resident equilibrium. By iteratively assessing whether a mutant can increase in frequency when rare, we can therefore characterize the long-term evolutionary process of successive allelic substitutions without tracking the full frequency dynamics.

Ecological dynamics

Consider a population structured into K discrete classes. These might be discrete habitats, ages, stages, sizes, or epidemiological states. For any pair of classes k and m, we assume that an individual of class m can contribute to class k; this contribution may be direct (via reproduction or class-transition) or indirect (via other classes). Such class structure is called irreducible (Caswell 2001; Stott et al. 2010).

To understand the model structure, we use a life-cycle graph (Caswell 2001), where vertices (nodes) represent classes and directed edges (paths) represent positive contribution via class-transition or births. The irreducibility assumption then means that the life-cycle graph is strongly connected: for any pair of classes, (k, m), there exists at least one finite-length path linking the vertices k and m.

The rate of change of class densities is modelled using a system of ordinary differential equations (ODEs):

$$\frac{\mathrm{d}\vec{N}}{\mathrm{d}t} = A\big(z \,\big|\, \vec{N}, z\big)\vec{N}, \tag{1}$$

where $\vec{N} = (N_1, \dots, N_K)^\top$ collects the class densities. For any given resident trait value z, we assume there exists a unique, globally stable ecological equilibrium $\vec{N^\circ} = (N_1^\circ, \dots, N_K^\circ)^\top$ with $N_k^\circ > 0$ a for all classes, $k = 1, 2, \dots, K$ and $A\Big(z \,\Big|\, \vec{N^\circ}, z\Big) = O$ (zero matrix). The potential existence of alternative equilibria or attractors does not affect our analysis, since the weak selection assumption prevents the population from converging to an alternative attractor (see Geritz et al. 2002; Priklopil & Lehmann 2020). Throughout this article, we assume that the resident population dynamics are regulated by sufficient negative density dependence at high densities, and that the population can grow at low densities. Under these standard ecological conditions, the resident dynamics admit a strictly positive, globally stable equilibrium (Cushing 1998). We refer to this globally stable monomorphic equilibrium as the resident equilibrium.

Dynamics of a rare mutant

Suppose a mutation arises with phenotype $z' = z + \delta$ (where $|\delta| \ll 1$). The density of this mutant in class k, denoted by N'_k, changes according to the following ordinary differential equations (ODEs):

$$\frac{\mathrm{d}N'_k}{\mathrm{d}t} = \sum_{m=1}^{K} a_{k,m}\Big(z' \,\Big|\, \vec{N}, \vec{N'}, z, z'\Big)N'_m, \quad k = 1, \dots, K, \tag{2}$$

where $a_{k,m}$ represents the per-capita rate at which class-m mutants contribute to the class-k mutant population. This rate depends on the environmental feedback generated by the densities and traits of both the resident and the mutant. Accordingly, the resident dynamics (Equation (1)) must also be augmented to account for the mutant density.

Assuming the mutant is initially rare, we can linearize the full joint system around the resident equilibrium, where the mutant is absent ($\vec{N'} = \vec{0}$). In this regime, the ability of the mutant to invade is governed by the linearized system:

$$\frac{\mathrm{d}\vec{N'}}{\mathrm{d}t} = J\vec{N'}. \tag{3}$$

Here, the Jacobian matrix J has entries $j_{k,m} \coloneqq a_{k,m}\big(z' \,\big|\, \vec{N}, \vec{0}, z, z'\big)$, which can be interpreted as the net rate at which class-m mutants produce class-k mutants in the resident environment. The invasion condition is determined by the spectral abscissa of J, denoted by $\sigma(J)$ (i.e., the largest real part among its eigenvalues). The mutant can successfully invade if $\sigma(J) > 0$, whereas it faces extinction if $\sigma(J) < 0$.

The primary difficulty with this direct approach is that the spectral abscissa, $\sigma(J)$, is often impossible to compute analytically. Although one might occasionally derive invasion conditions through ad-hoc algebraic manipulations, such as evaluating the sign of the determinant of J, these methods are typically highly model-specific. Furthermore, even when a closed-form invasion condition can be obtained, it frequently lacks a clear biological interpretation. Consequently, alternative, more systematic

approaches have been developed.

Most alternatives to directly analyzing $\sigma(J)$ involve shifting the timescale of the evolutionary dynamics. Rather than tracking the mutant population over absolute time (e.g., days or years), these approaches evaluate population change over an organismal generation. This concept is best illustrated using a simple unstructured population. Suppose the density of a mutant, n', changes according to the scalar ODE $\frac{\mathrm{d}n'}{\mathrm{d}t} = un' - vn'$, where u and v are the constant per-capita birth and death rates, respectively, and time is measured in days. The spectral abscissa is simply $\sigma = u - v$, which has units of days^{-1}. Invasion occurs if $u - v > 0$, meaning the daily fecundity exceeds the daily mortality. However, this inequality can be algebraically rearranged as $uv^{-1} > 1$. The left-hand side is now a dimensionless quantity, rendering it independent of the absolute time units. Biologically, because a mutant individual experiences a constant mortality rate v, its expected lifespan is v^{-1} days. Multiplying this expected lifespan by the daily offspring production rate, u, yields the dimensionless ratio uv^{-1}, which represents the expected total number of offspring a mutant individual will produce over its entire lifetime. If this lifetime reproductive output exceeds unity, the mutant population will grow and successfully invade.

While this unstructured example is simple enough that both invasion criteria ($\sigma > 0$ and $uv^{-1} > 1$) can be readily computed and biologically interpreted, introducing class structure significantly complicates the analysis. In multi-dimensional systems, the transition from continuous-time rates to generational reproductive output is far less straightforward, necessitating the formal mathematical machinery of the next-generation matrix.

Next-generation matrix (NGM)

The NGM method generalizes the concept of an individual's expected lifetime reproductive output to structured populations. This is achieved by constructing a matrix, G, whose entries $g_{k,m}$ represent the expected number of class-k offspring produced by a single class-m individual over its lifetime. To construct this matrix, we partition the continuous-time Jacobian as $J = U - V$. Here, U is a non-negative matrix capturing the inflow of new individuals (e.g., "births") into each class, while V captures all mortality and transition rates among the classes. From a mathematical standpoint, the biological labels assigned to these transitions are somewhat arbitrary, meaning the partitioning $J = U - V$ is not necessarily unique. Although we will explore the implications of this non-uniqueness later, any valid partition must satisfy three fundamental mathematical requirements: (i) $U \geq 0$, ensuring non-negative inflows; (ii) $\sigma(-V) < 0$, ensuring that in the absence of new inflows ($U = O$), the population densities asymptotically approach zero; and (iii) V^{-1} exists and is non-negative.

Under these conditions, the next-generation matrix is defined as $G \coloneqq UV^{-1}$. Hurford et al. (2010) formally demonstrated that

$$\sigma(J) \gtreqless 0 \quad \Longleftrightarrow \quad \rho(G) \gtreqless 1, \tag{4}$$

where $\rho(G)$ denotes the spectral radius of the NGM (i.e., its largest eigenvalue in modulus), and the notation $\gtreqless$ indicates that the inequalities strictly correspond across the equivalence. Consequently, the invasion condition can be evaluated equivalently using either $\sigma(J)$ or $\rho(G)$. It is straightforward to verify that the earlier scalar ODE example represents a special, one-dimensional case of this general result.

The primary advantage of the NGM framework is its capacity to yield simple, biologically interpretable invasion conditions that are often intractable when analyzing $\sigma(J)$ directly. Nevertheless, in high-dimensional systems or models with complex life cycles, deriving clear analytical results from the standard NGM remains challenging. While alternative simplification techniques exist—such as graph-theoretical decompositions (Rueffler et al. 2012; Rueffler & Metz 2013)—they are often mathematically demanding, which can limit their accessibility for applied modellers. A more direct strategy involves strategically choosing a non-standard decomposition $J = U - V$ that still satisfies the mathematical requirements but yields a simpler NGM, thereby facilitating biological interpretation. However, this strategy currently lacks a unifying theory, typically forcing researchers to rely on ad hoc, model-specific derivations.

In the following sections, we synthesize these disparate approaches into a unified framework that we term "structural evolutionary invasion analysis." This framework integrates two complementary tools: a generalized analysis of the invasion de-

terminant of G, and a systematic methodology for decomposing the Jacobian J. We call this approach "structural" because it exploits the algebraic architecture of the life cycle to characterize both short- and long-term evolutionary dynamics, entirely bypassing computationally demanding eigen-analyses. Ultimately, this framework serves as a systematic toolkit, empowering applied modellers to address complex evolutionary questions within the adaptive dynamics theory. To apply this framework, we rely on three standard assumptions typical of adaptive dynamics: (i) natural selection is weak; (ii) the resident equilibrium is globally asymptotically stable; and (iii) the resulting NGM is irreducible.

3 Synthesis: structural evolutionary invasion analysis

The structural evolutionary invasion analysis synthesizes several distinct approaches. Specifically, we integrate two complementary methods. The first method uses an algebraic approach (Appendix A): we calculate the determinant of matrices to capture the overall growth potential of a rare mutant lineage. This approach has remained underutilized in the literature, although it has appeared in previous works (e.g., Taylor & Bulmer 1980; Courteau & Lessard 2000; Day & Burns 2003; Metz & Leimar 2011; Rueffler et al. 2012). We refer to this quantity as the invasion determinant, highlighting both its mathematical nature as a determinant and its biological role in characterizing the invasion condition.

Second, to systematically reduce the dimension, we apply the Nonnegative Decomposition Theorem (proven in Appendix B; Box 1). This theorem guarantees that any biologically motivated decomposition—provided it satisfies mild non-negativity conditions—yields an NGM that preserves the correct invasion threshold. Based on this theoretical foundation, we introduce the Projected NGM (PNGM) approach (Appendix C). The PNGM builds on the theory of the type-reproduction number developed in theoretical epidemiology (Roberts & Heesterbeek 2003; Inaba & Nishiura 2008), focusing on the reproductive success of individuals in only a subset of classes while eliminating others. This reduces the model dimension and facilitates the calculation of the invasion condition. While algebraically this amounts to choosing a specific decomposition $J = U - V$, biologically it can be interpreted as approximating the mutant dynamics by a separation of timescales: 'slow' classes are retained while 'fast' classes are removed. From a life-cycle graph viewpoint, this effectively eliminates nodes from the original graph, as illustrated in Box 3. Crucially, this reduction preserves not only the invasion threshold but also Fisher's (1930) reproductive values of the retained classes, thus facilitating biological interpretation (Appendix C).

A further key property is that these methods preserve the (i) position of the evolutionary equilibrium, (ii) convergence stability towards it (Appendix D), and (iii) evolutionary stability against invasion of alternative mutants (Appendix D). These properties provide useful tools for predicting long-term evolutionary outcomes, extending beyond the analysis of instantaneous invasion conditions.

Key component 1: Invasion determinant

Throughout our analysis, we assume that selection is weak, consistent with the adaptive dynamics framework. As alluded to above, it is possible to obtain a condition on the determinant of a matrix that provides an invasion threshold as follows:

$$\rho(G) \gtreqless 1 \quad \Longleftrightarrow \quad -\det(I - G) \gtreqless 0 \tag{5}$$

(Appendix A). We refer to $-\det(I - G)$ as the invasion determinant. The invasion determinant provides an algebraically closed-form expression for the invasion condition, which provides a tractable and general tool for arbitrary, class-structured, populations. Although the basic idea underlying this method appears in earlier studies (Taylor & Bulmer 1980; Courteau & Lessard 2000; Day & Burns 2003; Metz & Leimar 2011; Rueffler et al. 2012), it has received limited attention in the literature and has been rarely used. To promote its practical utility, we here assign it a formal name and advocate its use as a systematic component of evolutionary invasion analysis.

Incidentally, we can also derive the invasion conditions using the original, continuous-time Jacobian:

$$\rho(G) \gtreqless 1 \quad \Longleftrightarrow \quad -\det(-J) \gtreqless 0 \tag{6}$$

(Appendix A), which has been also used in some studies (e.g., Day & Burns 2003; Hastings & Botsford 2006b; Boots & Best 2018).

One limitation of the invasion determinant approach is that it does not always yield biologically interpretable expressions. In particular, it does not account for Fisher's (1930) reproductive value – a crucial quantity that helps biological interpretations of outcomes of evolutionary invasion analysis. Despite this limitation, the method significantly simplifies the invasion condition and can thus facilitate theoretical analysis for evolutionary demography, with the advantage being more pronounced for complex or high-dimensional systems. Metz & Leimar (2011) further investigate the applicability of the invasion determinant and determine the condition for which we can relax the weak-selection assumption. This suggests that the invasion determinant can serve as a robust tool of deriving invasion condition beyond the traditional limit of adaptive dynamics theory.

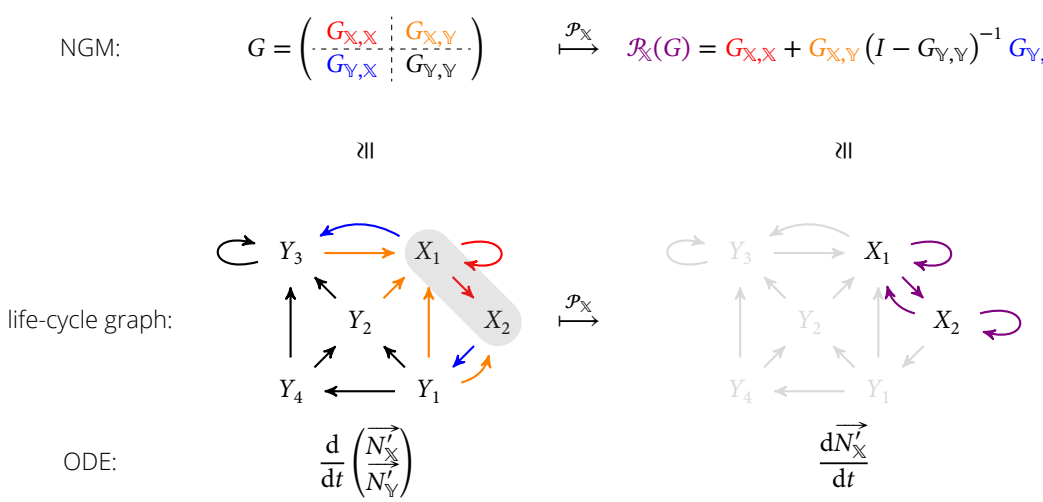

Figure 1: A schematic illustration of PNGM, with $\mathbb{X} = \{X_1, X_2\}$ for primary and $\mathbb{Y} = \{Y_1, Y_2, Y_3, Y_4\}$ for secondary groups. The colors: red for the pathway $[\mathbb{X} \leftarrow \mathbb{X}]$, orange for $[\mathbb{X} \leftarrow \mathbb{Y}]$, blue for $[\mathbb{Y} \leftarrow \mathbb{X}]$, and black for $[\mathbb{Y} \leftarrow \mathbb{Y}]$. Top panels depict linear-algebraic forms of the original next-generation matrix and PNGM. Bottom panels show the corresponding life-cycle graph (left) and its projection (right).

Key component 2: Projected Next-Generation Matrix (PNGM)

We refer to the next method as the projected NGM (PNGM) approach. We start with the above NGM G and partition the classes into two mutually exclusive groups: a 'primary' group and a 'secondary' group (Figure 1); for example, four classes can be divided into $\mathbb{X} = \{1, 2, 3\}$ and $\mathbb{Y} = \{4\}$ (where $\{\}$ is used for set notation; Figure 1). Such a grouping can be based on any biological feature of the classes.

Symbolically, we block-partition the NGM as:

$$G = \left(\begin{array}{c|c} G_{\mathbb{X},\mathbb{X}} & G_{\mathbb{X},\mathbb{Y}} \\ \hline G_{\mathbb{Y},\mathbb{X}} & G_{\mathbb{Y},\mathbb{Y}} \end{array}\right). \tag{7}$$

The two matrices in the diagonal blocks are square, and those in the off-diagonal blocks have compatible sizes. For example, when $G_{\mathbb{X},\mathbb{X}}$ is three-by-three and $G_{\mathbb{Y},\mathbb{Y}}$ is two-by-two, $G_{\mathbb{X},\mathbb{Y}}$ is three-by-two and $G_{\mathbb{Y},\mathbb{X}}$ is two-by-three. Biologically, each block matrix represents transfer of genes (either by reproduction or transition) among the primary and secondary groups. For

example, $G_{\mathbb{X},\mathbb{Y}}$ represents the transfer of genes from the secondary $\mathbb{Y}$ to primary $\mathbb{X}$ group.

Next, we consider how mutant individuals in the primary group (primary-group mutant) produce offspring in the primary group. There are two possibilities: (i) direct production, in which the primary mutants directly produce primary offspring during their lifetime. This process is captured by a loop-path $[\mathbb{X} \leftarrow \mathbb{X}]$, or algebraically by the submatrix $G_{\mathbb{X},\mathbb{X}}$. The other possibility is (ii) indirect production, in which primary mutants produce secondary offspring, and these secondary offspring then produce primary offspring at some point in the future. This occurs along a path from $\mathbb{X}$ to $\mathbb{X}$ via $\mathbb{Y}$, $[\mathbb{X} \leftarrow \mathbb{Y} \leftarrow \mathbb{X}]$. This process is represented by the matrix product $G_{\mathbb{X},\mathbb{Y}}G_{\mathbb{Y},\mathbb{X}}$. Following this logic, if we write P_n for the matrix whose elements give the total expected number of primary offspring produced by primary individuals within n generations ($n \geq 1$), we get:

$$P_n = G_{\mathbb{X},\mathbb{X}} + G_{\mathbb{X},\mathbb{Y}} \sum_{i=0}^{n-2} \left(G_{\mathbb{Y},\mathbb{Y}}\right)^i G_{\mathbb{Y},\mathbb{X}} \tag{8}$$

This interpretation suggests that whenever taking the limit $n \to \infty$ is possible, the following reduced-dimension matrix might be used to analyze invasion condition:

$$\mathcal{R}_{\mathbb{X}}(G) \coloneqq \lim_{n\to\infty} P_n = G_{\mathbb{X},\mathbb{X}} + G_{\mathbb{X},\mathbb{Y}} \left(I - G_{\mathbb{Y},\mathbb{Y}}\right)^{-1} G_{\mathbb{Y},\mathbb{X}}. \tag{9}$$

Most notably, P_n and $G_{\mathbb{X},\mathbb{X}}$ have the same size, and thus $\mathcal{R}_{\mathbb{X}}(G)$ is the projection of G onto a lower dimensional matrix whose classes are given by the primary group $\mathbb{X}$; the reader may note that while 'projection' in population demography often refers to an operator of population dynamics, here we use the term in the mathematical sense of 'dimensionality reduction'. In life-cycle graph, the projection corresponds to eliminating secondary groups and reallocating the paths (reproductive success) through secondary classes into primary classes (Figure 1). In other words, the projection method compresses the life-cycle graph.

Since the matrix $\mathcal{R}_{\mathbb{X}}(G)$ has a lower dimension, it is appealing to utilize this matrix as an alternative to the original NGM. Indeed, in Appendix C, we show that the limit always exists if selection is weak, and consequently prove the following equivalency:

$$\rho(G) \gtreqless 1 \quad \Longleftrightarrow \quad \rho(\mathcal{R}_{\mathbb{X}}(G)) \gtreqless 1. \tag{10}$$

The above result shows that the spectral radius of the reduced matrix $\mathcal{R}_{\mathbb{X}}(G)$ provides an alternative invasion condition. We refer to $\mathcal{R}_{\mathbb{X}}(G)$ as projected next-generation matrix, or PNGM of G. This is referred to as the type-reproduction number in theoretical epidemiology (Roberts & Heesterbeek 2003).

The PNGM may be also derived using the original NGM framework. We first decompose the Jacobian as $J = U - V$, with block matrices $J_{\mathbb{X},\mathbb{X}} = U_{\mathbb{X},\mathbb{X}} - V_{\mathbb{X},\mathbb{X}}$, $J_{\mathbb{X},\mathbb{Y}} = U_{\mathbb{X},\mathbb{Y}}$, $J_{\mathbb{Y},\mathbb{X}} = U_{\mathbb{Y},\mathbb{X}}$, and $J_{\mathbb{Y},\mathbb{Y}} = U_{\mathbb{Y},\mathbb{Y}} - V_{\mathbb{Y},\mathbb{Y}}$, and write $G = UV^{-1}$ for the resulting NGM, where we write $G_{\mathbb{X},\mathbb{Y}} = U_{\mathbb{X},\mathbb{Y}}V_{\mathbb{Y},\mathbb{Y}}^{-1}$ etc.; we note that this decomposition satisfies the hypotheses of the theorem of NGM. On the other hand, we consider another decomposition and the resulting NGM as follows:

$$\widetilde{U} = \left(\begin{array}{c:c} U_{\mathbb{X},\mathbb{X}} & U_{\mathbb{X},\mathbb{Y}} \\ \hdashline O & O \end{array}\right), \quad \widetilde{V} = \left(\begin{array}{c:c} V_{\mathbb{Y},\mathbb{Y}} & O \\ \hdashline -U_{\mathbb{Y},\mathbb{X}} & -(U_{\mathbb{Y},\mathbb{Y}} - V_{\mathbb{Y},\mathbb{Y}}) \end{array}\right), \quad \widetilde{G} = \widetilde{U}\widetilde{V}^{-1} = \left(\begin{array}{c:c} \mathcal{R}_{\mathbb{X}}(G) & * \\ \hdashline O & O \end{array}\right) \tag{11}$$

where the asterisk is some matrix. As a result, $\rho(\widetilde{G}) = \rho(\mathcal{R}_{\mathbb{X}}(G))$. Hence, PNGM can be regarded as an outcome of NGM with different decomposition of the Jacobian. Box 1 describes more technical details to clarify the NGMs that have the same invasion condition.

Properties of the framework

Beyond the invasion condition itself, the present framework possesses several, biologically useful properties (summarized in Box 3). First, the dimensionality reduction via the PNGM is mathematically equivalent to a separation of timescales, where the eliminated (secondary) classes are assumed to equilibrate instantaneously relative to the retained (primary) classes (Appendix C). Second, despite this reduction, the reproductive values of the retained classes are preserved (but only to the first order effect

of selection; Appendix C). Finally, the framework preserves not only the invasion threshold (i.e., whether the spectral radius exceeds one) but also local stability properties around the equilibrium, thereby enabling the analysis of long-term consequence of evolutionary dynamics (e.g., convergence and evolutionary stability; Appendix D and E).

Summary of the framework

We have provided key two methods: the invasion determinant and decomposition analysis. By exploiting the flexible decomposability of the NGM and integrating the determinant formula with PNGM, we are able to generalize invasion analysis to higher-dimensional class-structured systems. The invasion determinant is an algebraic tool of writing down the invasion condition in closed form. The decomposition analysis allows us to partition NGM into two nonnegative matrices and calculate an alternative NGM based on the decomposition. The most notable application of the decomposition analysis includes the PNGM to calculate the type-reproduction number. These methods can be also used to locate candidate evolutionary equilibrium and its stability conditions (convergence- and evolutionary stability). One may preferably use any of the unifying methods. The structural evolutionary invasion analysis may allow for systematic evaluation and prediction of evolutionary dynamics in structured populations. Some useful techniques are encapsulated in Box 2.

In practice, the invasion determinant and PNGM serve complementary purposes, and the choice between them is best guided by the modelling goal. If the primary objective is analytical manipulation, differentiation, or stability calculations (e.g., selection gradients, convergence stability, or evolutionary stability), the invasion determinant is often preferable because it yields a scalar condition that can be differentiated and simplified systematically. In contrast, if the goal is biological interpretation, PNGM is typically more useful because it retains a clear life-cycle meaning and preserves reproductive-value weighting on the retained (primary) classes, thereby clarifying which classes and pathways contribute most to mutant success. The main practical challenge in using PNGM is choosing primary and secondary groups. We recommend selecting primary groups to match the biological question (typically the birth or transmission classes of interest) and treating as secondary those classes that act as transient intermediates. When multiple admissible partitions exist, one can choose the partition that yields the most interpretable or tractable reduced matrix, since the invasion threshold is invariant under these reductions.

4 Examples

We demonstrate our methodology with four examples. More detailed analyses are encapsulated in Appendix E. The first two models use continuous time dynamics, while the last two use discrete time dynamics. We briefly explain the procedure of invasion analysis for discrete time models in the third example.

Example 1: Two-class model

We first examine a two-class model since it provides the simplest, non-trivial example. We consider a stage-structured population with semi-adult and adult stages, both reproductive. The mutant dynamics read:

$$\begin{aligned} \frac{\mathrm{d}N_1'}{\mathrm{d}t} &= b_1'N_1' + b_2'N_2' - (a_1' + m_1)N_1' \\ \frac{\mathrm{d}N_2'}{\mathrm{d}t} &= a_1'N_1' - m_2N_2', \end{aligned} \tag{13}$$

where we have written parameters (each with a subscript) b' for fecundity, which may be subject to density-dependent reduction; a' for transition; and m for mortality. Note that we have already substituted the resident equilibrium into the model. This example is relevant to models such as epidemiological susceptible-infected dynamics with host evolution, or source-sink metapopulation dynamics. We can use the primed parameters a's or b's for evolving trait(s), where these traits are traded-off against each other.

The Jacobian of the mutant dynamics can be partitioned as:

$$J = \underbrace{\begin{pmatrix} b_1' & b_2' \\ 0 & 0 \end{pmatrix}}_{=B} + \underbrace{\begin{pmatrix} 0 & 0 \\ a_1' & 0 \end{pmatrix}}_{=T^{\text{in}}} - \underbrace{\begin{pmatrix} a_1' & 0 \\ 0 & 0 \end{pmatrix}}_{=T^{\text{out}}} - \underbrace{\begin{pmatrix} m_1 & 0 \\ 0 & m_2 \end{pmatrix}}_{=M}, \tag{14}$$

where from left to right, the matrices represent birth, transition-in, transition-out, and mortality. We write, dropping the prime symbol for brevity, $f_1 = b_1'/(a_1' + m_1)$ and $f_2 = b_2'/m_2$ for the expected reproductive outputs in stage 1 and 2, and $s = a_1'/(a_1' + m_1')\,(< 1)$ for survival probability. Using these symbols, we can either decompose the Jacobian as (i) $U = B$, where the inflow term includes birth only; or (ii) $U = B + T^{\text{in}}$, where the inflow term includes transitions. To demonstrate the generality of the framework, we take $U = B + T^{\text{in}} - T^{\text{out}}$ and $V = M$ to get:

$$G = \underbrace{\begin{pmatrix} f_1 - s & f_2 \\ s & 0 \end{pmatrix}}_{=H_1} \underbrace{\left(\begin{pmatrix} 1 & 0 \\ 0 & 1 \end{pmatrix} - \begin{pmatrix} s & 0 \\ 0 & 0 \end{pmatrix} \right)^{-1}}_{=(I-H_2)^{-1}} = \begin{pmatrix} \frac{f_1 - s}{1-s} & f_2 \\ \frac{s}{1-s} & 0 \end{pmatrix}. \tag{15}$$

This matrix is not nonnegative when $f_1 < s$ (which occurs for instance when the class-1 individual does not reproduce), and may not be biologically relevant. However, this matrix has nonnegative off-diagonals (called as 'Metzler matrix' or 'essentially nonnegative matrix'), and has similar properties to those of nonnegative matrices (Berman & Plemmons 1987). Indeed, taking PNGM with $\mathbb{X} = \{1\}$ yields $\rho(\mathcal{R}_{\mathbb{X}}(G)) = w_1 := (f_1 + sf_2 - s)/(1 - s)$, which we can rearrange as the invasion condition $w_2 := f_1 + sf_2 > 1$. Overall, we have essentially two formulas for invasion fitness: $w_1 = (f_1 + sf_2 - s)/(1 - s), and w_2 = f_1 + sf_2$.

More generally, the invasion condition for two-class models can be further simplified to:

$$\rho(G) \gtreqless 1 \quad \Longleftrightarrow \quad g_{1,1} + g_{2,2} - \left(g_{1,1}g_{2,2} - g_{1,2}g_{2,1}\right) = \text{tr}(G) - \det(G) \gtreqless 1, \tag{16}$$

which is useful for practical analyses for two-class models (e.g., Rodrigues & Gardner 2013; Massol & Débarre 2015; Iritani et al. 2019). There does not exist analogous formula when the system is three or higher dimensional.

We now examine the selection gradient, defined as the first derivative of the invasion fitness with respect to the mutant phenotypic deviation δ. While both w_1 and w_2 yield identical stability properties, we proceed with w_2 due to its algebraic simplicity. Applying the differentiation technique outlined in Box 3, assuming that f_1, s, and f_2 all depend on the mutant phenotype $z' = z + \delta$, yields:

$$\left.\frac{\partial w_2}{\partial \delta}\right|_{\delta=0} = f_1^\circ \cdot \frac{f_1^{(1)}}{f_1} + s^\circ f_2^\circ \cdot \left(\frac{s^{(1)}}{s} + \frac{f_2^{(1)}}{f_2} \right). \tag{17}$$

Recalling that the neutrality condition implies $w_2^\circ = f_1^\circ + s^\circ f_2^\circ = 1$, the selection gradient can be rewritten by substituting $s^\circ f_2^\circ = 1 - f_1^\circ$:

$$\left.\frac{\partial w_2}{\partial \delta}\right|_{\delta=0} = f_1^\circ \cdot \frac{f_1^{(1)}}{f_1^\circ} + (1 - f_1^\circ) \cdot \left(\frac{s^{(1)}}{s^\circ} + \frac{f_2^{(1)}}{f_2^\circ} \right). \tag{18}$$

This expression offers a clear biological interpretation: the total selection gradient is a weighted sum of the marginal changes in life-history traits. Specifically, the weights f_1° and $1 - f_1^\circ$ correspond to the relative reproductive contributions of the class 1 (direct reproduction) and class 2 (survival and reproduction) pathways to the next generation at the resident equilibrium. As such, the selection gradient captures the effect of natural selection throughout individual life-cycle. An analogous analysis is possible for the alternative fitness function w_1, although the resulting expression may look more complex at first sight.

While we focus here on the selection gradient (convergence stability), the second derivative required for assessing evolutionary stability can be derived in an equally straightforward manner using w_2. This avoids the complexity of differentiating the eigenvalues of the original matrix (see Appendix D for the theoretical guarantee).

To summarize, this two-class example demonstrates that the structural evolutionary invasion analysis yields the same in-

vasion condition across various types of biologically motivated decompositions of NGM. It also highlights the generality of the decomposition theorem, in which NGM need not be nonnegative and can be used as an alternative NGM with the same invasion condition.

Example 2: Evolutionary epidemiological model

The second, continuous-time example is based on the model of sex-structured epidemiological dynamics studied in Mitchell et al. (2022). While the authors have considered the coevolution between the virulence of vertically transmitting pathogen and sex-specific host recovery, we focus on host evolution for illustration.

We describe the mutant dynamics as:

$$\begin{aligned}
\frac{\mathrm{d}S'_\mathrm{f}}{\mathrm{d}t} &= \theta_\mathrm{ff} b'_\mathrm{f} \cdot \frac{S^\circ_\mathrm{m} + I^\circ_\mathrm{m}}{N^\circ_\mathrm{T}} \cdot (S'_\mathrm{f} + (1-\nu) I'_\mathrm{f}) + \theta_\mathrm{fm} b'_\mathrm{m} \cdot \frac{S'_\mathrm{m} + I'_\mathrm{m}}{N^\circ_\mathrm{T}} \cdot (S^\circ_\mathrm{f} + (1-\nu) I^\circ_\mathrm{f}) + \gamma'_\mathrm{f} I'_\mathrm{f} - h S'_\mathrm{f} - \mu S'_\mathrm{f} \\
\frac{\mathrm{d}I'_\mathrm{f}}{\mathrm{d}t} &= \theta_\mathrm{ff} b'_\mathrm{f} \cdot \frac{S^\circ_\mathrm{m} + I^\circ_\mathrm{m}}{N^\circ_\mathrm{T}} \cdot \nu I'_\mathrm{f} + \theta_\mathrm{fm} b'_\mathrm{m} \cdot \frac{S'_\mathrm{m} + I'_\mathrm{m}}{N^\circ_\mathrm{T}} \cdot \nu I^\circ_\mathrm{f} + h S'_\mathrm{f} - \left(\mu + \gamma'_\mathrm{f} + \alpha_\mathrm{f}\right) I'_\mathrm{f} \\
\frac{\mathrm{d}S'_\mathrm{m}}{\mathrm{d}t} &= \theta_\mathrm{mf} b'_\mathrm{f} \cdot \frac{S^\circ_\mathrm{m} + I^\circ_\mathrm{m}}{N^\circ_\mathrm{T}} \cdot (S'_\mathrm{f} + (1-\nu) I'_\mathrm{f}) + \theta_\mathrm{mm} b'_\mathrm{m} \cdot \frac{S'_\mathrm{m} + I'_\mathrm{m}}{N_\mathrm{T}} \cdot (S^\circ_\mathrm{f} + (1-\nu) I^\circ_\mathrm{f}) + \gamma'_\mathrm{m} I'_\mathrm{m} - h S'_\mathrm{m} - \mu S'_\mathrm{m} \\
\frac{\mathrm{d}I'_\mathrm{m}}{\mathrm{d}t} &= \theta_\mathrm{mf} b'_\mathrm{f} \cdot \frac{S^\circ_\mathrm{m} + I^\circ_\mathrm{m}}{N^\circ_\mathrm{T}} \cdot \nu I'_\mathrm{f} + \theta_\mathrm{mm} b'_\mathrm{m} \cdot \frac{S'_\mathrm{m} + I'_\mathrm{m}}{N^\circ_\mathrm{T}} \cdot \nu I^\circ_\mathrm{f} + h S'_\mathrm{m} - (\mu + \gamma'_\mathrm{m} + \alpha_\mathrm{m}) I'_\mathrm{m}.
\end{aligned} \tag{19}$$

where $S^\circ_\mathrm{f}, I^\circ_\mathrm{f}, S^\circ_\mathrm{m}$, and I°_m are the resident equilibrium densities of susceptible female, infected female, susceptible male, and infected male, respectively. In this system of equations, we write b for birth (subscript f for maternity and m for paternity), as a function of recovery rate (fertility cost of recovery) and also the densities of the resident (density-dependent death and effective population size); θ for gene transmission between sexes (for example, all θs are one-half for diploid organisms); ν for vertical transmission; γ for recovery; $h = \beta(I^\circ_\mathrm{f} + I^\circ_\mathrm{m})$ for the force of infection (with β transmission rate); μ for natural death; and α for virulence. Parameters are sex-specific except for (i) vertical transmission (ν) which occurs only from infected female and (ii) natural death rate μ which is common for both sexes.

The Jacobian is a four-by-four matrix, with the (4, 1)-st element (creation of I'_m by S'_f) being zero. We put only birth terms into U while all the others into V (including infection, recovery and mortality):

$$J = \left(\begin{array}{c:c} U_\mathrm{ff} & U_\mathrm{fm} \\ \hdashline U_\mathrm{mf} & U_\mathrm{mm} \end{array}\right) - \left(\begin{array}{c:c} V_\mathrm{f} & O \\ \hdashline O & V_\mathrm{m} \end{array}\right), \quad G = \left(\begin{array}{c:c} U_\mathrm{ff} & U_\mathrm{fm} \\ \hdashline U_\mathrm{mf} & U_\mathrm{mm} \end{array}\right) \left(\begin{array}{c:c} V_\mathrm{f}^{-1} & O \\ \hdashline O & V_\mathrm{m}^{-1} \end{array}\right) = \left(\begin{array}{c:c} \theta_\mathrm{ff} G_\mathrm{f} & \theta_\mathrm{fm} G_\mathrm{m} \\ \hdashline \theta_\mathrm{mf} G_\mathrm{f} & \theta_\mathrm{mm} G_\mathrm{m} \end{array}\right) \tag{20}$$

where G_f and G_m are fitness components of female and male, respectively, ignoring the genetic inheritance system. We can immediately see that G has rank two (Mitchell et al. 2022, Eqn 10b), i.e., the model is effectively two-dimensional.

We now explore the formula of invasion fitness for diploidy and haplodiploigy separately. We find that, for diploidy:

$$G = \frac{1}{2} \left(\begin{array}{c:c} G_\mathrm{f} & G_\mathrm{m} \\ \hdashline G_\mathrm{f} & G_\mathrm{m} \end{array}\right). \tag{21}$$

Using the method in Box 1, we get the simple invasion condition $\rho(G_\mathrm{f}/2 + G_\mathrm{m}/2) > 1$. That is, essentially the NGM is given by the arithmetic mean of sex-specific NGMs. Note that G_f and G_m are both two-by-two, and so the two-class model results are readily applicable to obtain the invasion condition. Meanwhile, the simple arithmetic-mean formula breaks down for haplodiploidy, leading to the invasion condition $\rho(G_\mathrm{f}/2 + G_\mathrm{m} G_\mathrm{f}/2) > 1$ (Appendix E). Biologically, this multiplicative term ($G_\mathrm{m} G_\mathrm{f}$) explicitly captures the asymmetric nature of gene transmission: a male's reproductive success is strictly bottlenecked by the fitness of females in the previous generation. Consequently, this structural derivation immediately predicts a fundamental asymmetry in intralocus sexual conflict; traits that benefit males at the expense of females (i.e., high G_m but low G_f) are strongly selected against. Our framework thus transparently demonstrates how genetic systems inherently bias sex-specific

life-history evolution (such as sex-specific recovery or immunity) toward female optima, without the need to solve complex multi-generation recursions.

Example 3: Discrete-time Lefkovitch model

The above examples focus on continuous-time population dynamics and thus do not cover discrete-time models. Applications of discrete-time evolutionary dynamics include numerous traits – for example, dispersal (Hamilton & May 1977; Taylor 1988; Iritani & Iwasa 2014), mating system in plants (Lande & Schemske 1985; Iritani & Cheptou 2017), sex ratios (Hamilton 1967; Bulmer & Taylor 1980; Frank 1987; Iritani et al. 2021), and social behaviors (Taylor 1992; Rodrigues & Gardner 2012; Iritani 2020). For discrete-time models, the population dynamics of the mutant linearized around the resident equilibrium is given by:

$$\overrightarrow{N'}(t+1) = J^{\mathrm{D}}\overrightarrow{N'}(t), \tag{22}$$

where J^{D} represents the Jacobian (^{D} for 'discrete-time'), and also satisfies the mathematical conditions of a NGM. The invasion condition is thus given by $\rho\left(J^{\mathrm{D}}\right) = \rho(G) > 1$.

We use the result above to analyze Lefkovitch's (1965) model, which helps us understand the biological meaning of PNGM. We consider one juvenile stage (state 1) and three adult stages (states 2, 3 and 4), in which all adults are reproductively mature. We first construct the NGM apply PNGM by partitioning the classes as $\mathbb{X} = \{1, 2, 3\}$ and $\mathbb{Y} = \{4\}$ (Figure 2):

$$G := \left(\begin{array}{ccc:c} g_{1,1} & g_{1,2} & g_{1,3} & g_{1,4} \\ g_{2,1} & g_{2,2} & 0 & 0 \\ 0 & g_{3,2} & g_{3,3} & 0 \\ \hdashline 0 & 0 & g_{4,3} & g_{4,4} \end{array}\right) \longmapsto \quad \mathcal{P}_{\mathbb{X}}(G) = \begin{pmatrix} g_{1,1} & g_{1,2} & \widehat{g_{1,3}} \\ g_{2,1} & g_{2,2} & 0 \\ 0 & g_{3,2} & g_{3,3} \end{pmatrix}. \tag{23}$$

We can immediately see that in this example, PNGM modifies the $(1, 3)$-rd element as $\widehat{g_{1,3}} = g_{1,3} + g_{1,4}(1 - g_{4,4})^{-1} g_{4,3}$, where the second additional term represents the reproductive success of an individual in class 3 via class 4, assuming that the population dynamics in class-4 is at quasi-equilibrium (Figure 2). In general, PNGM allows the removal of intermediate classes from life-cycle graphs by appropriately redistributing their per capita contributions to other reproductive pathways (e.g., 3 to 1). This effectively compresses the life-cycle graph (i.e., matrix) while preserving the overall lifetime reproductive success.

In Appendix E, we show that the invasion condition reads:

$$\sum_{m=1} f_m \prod_{k=1}^{m} s_k > 1, \tag{24}$$

where s_k represents the survival probability of an individual in class k. Equation (24) represents the canonical form of reproductive success: fitness is survival times fecundity. Rueffler & Metz (2013) investigate the condition for which the reproductive success may be expressed in this canonical form (see Theorem 3 therein).

To further examine the long-term evolutionary outcomes, one may differentiate the left hand side of this invasion condition, using the techniques given in Box 2. The resulting formula can be interpreted as Fisher's (1941) average excess and thus yields a biologically transparent expression linking the effects of selection and pleiotropy (mutation influencing multiple phenotypes expressed at different stages).

For ecological or epidemiological models, Hastings & Botsford (2006a), Rueffler et al. (2012), and Lewis et al. (2019) have rationalized this calculation by decomposing life-cycle graphs into sub-structures with distinct pathways of reproductive outputs. These authors' methods, however, require a careful treatment of signs (plus or minus. See Hastings & Botsford 2006a, Eqn 2). On the other hand, applying the PNGM or invasion determinant automatically solves this problem because these calculations only require solving linear equations or equivalently computing the determinant, which can be easily coded in standard computational software.

$$G := \left(\begin{array}{ccc|c} g_{1,1} & g_{1,2} & g_{1,3} & g_{1,4} \\ g_{2,1} & g_{2,2} & 0 & 0 \\ 0 & g_{3,2} & g_{3,3} & 0 \\ \hline 0 & 0 & g_{4,3} & g_{4,4} \end{array}\right) \cong$$

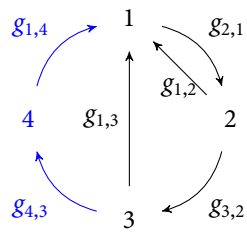

$$\mathcal{R}_{\mathbb{X}}(G) = \left(\begin{array}{ccc} g_{1,1} & g_{1,2} & \widehat{g_{1,3}} \\ g_{2,1} & g_{2,2} & 0 \\ 0 & g_{3,2} & g_{3,3} \end{array}\right) \cong$$

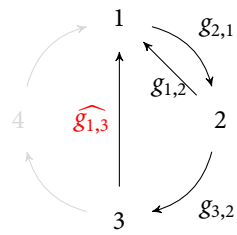

$$\left(\widehat{g_{1,3}} = g_{1,3} + \underbrace{g_{1,4} \cdot \left(1 - g_{4,4}\right)^{-1} \cdot g_{4,3}}_{[1 \leftarrow 4 \leftarrow 3]}\right)$$

Figure 2: Lefkovitch model. Top: the original NGM G and corresponding life-cycle graph. Self-loops are not shown for simplicity. Bottom: PNGM and resulting life-cycle graph. We see $g_{1,3}$ is changed to $g_{1,3} + g_{1,4}\left(1 - g_{4,4}\right)^{-1} g_{4,3}$, which means that the reproductive pathway from class-3 to class-1 now accounts for the reproductive pathway via class-4.

Example 4: Dispersal in stable habitats

We analyze the evolutionary model of dispersal in a saturated metapopulation (Hamilton & May 1977). The metapopulation consists of an infinitely many number of patches each occupied by the same number, K, of reproductive adults, following Wright's (1931) island-model of dispersal. For demography, we use the 'birth-death Moran process': all individuals produce the same number of offspring, and one individual is replaced by the newborn after natal dispersal of the offspring, where dispersal rate is d with mortality cost to dispersal c. Such replacement is based on random competition among offspring present in the patch to choose one individual, forming the next generation. All other offspring die.

We now consider the evolution of dispersal rate and introduce a mutant dispersal $d' = d + \delta$ under weak selection (i.e., δ is small). Writing $k = 1, \ldots, K$ for the number of mutants in a patch, the transition probability $S'_{m,k}$ from class k to m is given by:

$$S'_{m,k} = \begin{cases} \phi'_k & = \dfrac{K-k}{K} \cdot \dfrac{k(1-d')}{k(1-d') + (K-k)(1-d) + K(1-c)d} & \text{if} \quad m = k+1, k \neq 0; \\ \mu'_k & = \dfrac{k}{K} \cdot \dfrac{(K-k)(1-d) + K(1-c)d}{k(1-d') + (K-k)(1-d) + K(1-c)d} & \text{if} \quad m = k-1; \\ 1 - \phi'_k - \mu'_k & & \text{otherwise} \end{cases} \tag{25}$$

(Ewens 2004), with conventionally $\phi'_0 := (1-c)d'/(K(1-cd))$, the probability that a patch with no mutant individual becomes a patch with 1 mutant. Using the transition probabilities in Equation (25) gives the discrete-time stochastic process, of:

$$\begin{aligned} q'_1(t+1) &= q'_1(t) + \phi'_0 \sum_{m=1}^{K} m q'_m(t) + \mu'_2 q'_2(t) - (\phi'_1 + \mu'_1)\, q'_1(t), \\ &\vdots \\ q'_k(t+1) &= q'_k(t) + \mu'_{k+1} q'_{k+1}(t) + \phi'_{k-1} q'_{k-1}(t) - \left(\phi'_k + \mu'_k\right) q'_k(t), \\ &\vdots \\ q'_K(t+1) &= q'_K(t) + \phi'_{K-1} q'_{K-1}(t) - \mu'_K q'_K(t), \end{aligned} \tag{26}$$

where $q'_k(t)$ represents the proportion of patches with k mutants, conditioned that at least one mutant is present, at time t, $k = 1, 2, \dots, K$. The invasion condition is given by $\rho(G) = \sum_{m=1}^{K} m \prod_{k=1}^{m} (\phi'_{k-1}/\mu'_k)$ (Mullon & Lehmann 2014), as is consistent with the metapopulation-fitness concept (Metz & Gyllenberg 2001; Ajar 2003; Massol et al. 2009; Mullon et al. 2016).

We recover the invasion condition by recursively applying the timescale separation to Equation (26). We see that the dynamics of class-K depends only on those of K and $K-1$. We therefore first solve $q'_K(t+1) = q'_K(t)$ to eliminate q'_K and get $q'_K = q'_{K-1}\phi'_{K-1}/\mu'_K$. Next, we solve $q'_{K-1}(t+1) = q'_{K-1}(t)$ to eliminate q'_{K-1}. Combining these results, we eliminate q'_K and q'_{K-1}. Recursively, we get $q'_m = q'_1 \prod_{k=1}^{m-1} (\phi'_k/\mu'_{k+1})$ for $m = 2, \dots, K$. Substituting these into the first line of Equation (26) yields:

$$q'_1(t+1) - q'_1(t) = \phi'_0 \sum_{m=1}^{K} m q'_1(t) \prod_{k=1}^{m-1} \frac{\phi'_k}{\mu'_{k+1}} - \mu'_1 q'_1(t) = \left(\sum_{m=1}^{K} m \prod_{k=1}^{m} \frac{\phi'_{k-1}}{\mu'_k} - 1 \right) \mu'_1 q'_1(t). \tag{27}$$

Thus the invasion condition is given by $\sum_{m=1}^{K} m \prod_{k=1}^{m} (\phi'_{k-1}/\mu'_k) > 1$ as desired. This invasion condition is similar to Equation (24) in the Lefkovitch model, due to the product term representing the sojourn time in each state. We can also derive the explicit formula of the selection gradient by evaluating the number of generations a patch spends possessing k mutants until the extinction of the mutant lineage (Mullon et al. 2016).

This example demonstrates that recursive operations of the quasi-equilibrium approximation may simplify the problem in some cases. The quasi-equilibrium approximation is especially useful when NGM is tri-diagonal, which occurs for stage-structured models or Moran processes. However, using other models (say Wright-Fisher process) would make the analysis more complex (Ajar 2003). Yet, it often suffices to examine the first or second derivative of the invasion condition. For this purpose, we can make use of properties of matrix derivatives. More details are presented in Box 2 and Appendix D.

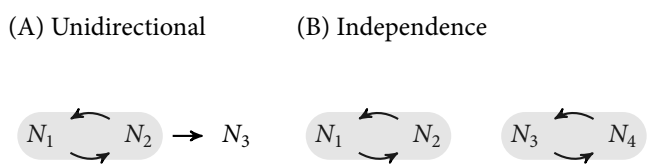

Figure 3: Two typical examples of reducible life-cycle graphs (i.e., non-irreducible life-cycles). Arrows represent transitions between classes, and gray bands highlight subsets of classes that form irreducible components — subgraphs in which every node is reachable from any other within the same component. In both examples, the invasion-implies-substitution principle fails: a mutation arising in class 3, for instance, cannot spread to fix in the entire population in both panels: (A) Classes 1 and 2 are interconnected, allowing gene flow between them. However, no gene flow from class 3 to class 2 is possible. Thus a mutant emerging in class 3 will never get fixated. (B) Classes 1 and 2 form one interconnected group, and classes 3 and 4 form another. There is no gene flow between these two groups, resulting in two isolated irreducible components. Again, fixation is impossible.

5 Discussion

We have synthesized a general, unifying framework of evolutionary invasion analysis for class-structured populations. This synthesis integrates two main approaches, the invasion determinant and the projected next-generation matrix (PNGM). The invasion determinant provides a determinant-based formula for invasion fitness (Taylor & Bulmer 1980). We also show that the PNGM method has biologically clear interpretations (Box 3): (i) Fisher's (1930) reproductive values remain invariant under this transformation, and (ii) PNGM results from a separation of dynamical timescales among classes. These advantages are illustrated in four examples. Beyond invasion conditions, these methods also allow us to derive long-term, stability properties of evolutionary equilibrium (Box 3). Illustrative examples demonstrate the utility of this framework, with practical protocols for two-class models (Example 1). Example 2 of evolutionary epidemiology highlights that even when the full Jacobian is complex (four-by-four), the structural approach can decompose the invasion fitness into interpretable sex-specific components. The

framework is readily applicable to both continuous-time and discrete-time dynamics (Example 3), including spatially structured model (Example 4). Collectively, the structural evolutionary invasion analysis provides a systematic tool for analyzing invasion conditions within the adaptive dynamics theory.

The invasion determinant, originally formulated by Taylor & Bulmer (1980) (see also Courteau & Lessard 2000; Rueffler et al. 2012), provides a general algebraic tool to derive invasion conditions. Our derivation relies crucially on the assumption of weak selection, where the phenotypic effect of a mutation is small. This assumption, however, is not highly restrictive; it often provides a robust approximation for evolutionary dynamics (Mullon & Lehmann 2014) and can be formally relaxed, particularly for continuous quantitative traits (for precise details, see Metz & Leimar 2011). Furthermore, the invasion determinant facilitates the derivation of higher-order properties, such as the stability of evolutionary equilibria, and serves as the mathematical foundation for the negative decomposition theorem (which yields the projected next-generation matrix). Thus, while the bare determinant might sometimes lack immediate biological transparency, it constitutes the analytical core of structural evolutionary invasion analysis.

The projected next-generation matrix (PNGM) systematically simplifies life-cycle graphs by eliminating secondary classes. While this method builds upon the type-reproduction number theory from epidemiology (Roberts & Heesterbeek 2003), our synthesis highlights two crucial biological insights for evolutionary demography (Box 3). First, constructing a PNGM is mathematically equivalent to separating the timescales of class dynamics. This equivalence is particularly advantageous in high-dimensional systems—as demonstrated in the metapopulation model (Example 4)—because it reduces complex matrix problems to tractable scalar or low-dimensional conditions. It allows researchers to place any subset of classes into a quasi-equilibrium state without requiring an actual, physiological separation of timescales. As illustrated by the Lefkovitch model (Example 3), removing intermediate stages transparently exposes the net reproductive pathways. Second, the PNGM preserves Fisher's (1930) reproductive values for the retained classes. In structured populations, variations in how different classes transmit alleles (nonheritable class transmission) complicate the evaluation of allele-frequency changes (Taylor 1990; Frank 1998; Rousset 2004; Priklopil & Lehmann 2020, 2024). By employing this structural reduction, we demonstrate that tracking gene-frequency changes strictly within the focal subset is sufficient to determine mutant invasibility. This implies that transient class transmission dynamics can be safely bypassed when evaluating initial invasion. Therefore, applying the PNGM to evolutionary dynamics provides conceptual clarity, not merely a mathematical shortcut.

The theory of evolutionary demography aims to understand how complex demographic structures shape patterns of adaptation (Takada & Nakajima 1992; Cushing 1998; Takada & Nakajima 1998; Easterling et al. 2000; Caswell 2001; Tuljapurkar et al. 2003). Over the past decade, integral projection models (IPMs) have emerged as powerful tools in this field (Ellner et al. 2016; Rees & Ellner 2016). IPMs incorporate continuous traits, such as size, weight, or age, into the adaptive dynamics framework, allowing for a realistic representation of individual heterogeneity. These models typically use an integral operator rather than a finite matrix for the NGM, resulting in an infinite-dimensional system. Nevertheless, the core logic of the PNGM framework remains robust for two reasons. First, the corresponding task of the PNGM in IPMs is simply to partition the physiological space into two regions and compute an effective operator for the primary region; this concept has already been integrated into epidemiological studies (Inaba & Nishiura 2008). Second, in practice, IPMs are numerically implemented by discretizing the continuous state space into a finite number of classes. This numerical scheme immediately reduces the problem to the standard, matrix-based domain. Thus, our approach offers a principled way to extend evolutionary invasion analysis into the IPM framework, potentially improving the tractability and interpretability of extended IPMs.

Beyond lifetime reproductive success, the present framework facilitates the determination of long-term evolutionary consequences, namely convergence stability and evolutionary stability (Maynard Smith & Price 1973; Maynard Smith 1982; Christiansen 1991; Takada & Kigami 1991; Eshel 1996). Such stability analyses require the first and second partial derivatives of the invasion fitness with respect to phenotypes. Difficulty typically arises when the population comprises many classes, as the analytical differentiation of the leading eigenvalue becomes computationally prohibitive and requires explicit information on the reproductive values of all classes (e.g., Avila & Mullon 2023). In this context, our framework offers two complementary pathways to overcome this high-dimensional hurdle. For algebraic or computational purposes, one can directly differentiate

the invasion determinant (Appendix D). This approach is often more straightforward than differentiating the spectral radius itself, as it avoids the explicit calculation of eigenvectors. Alternatively, when interpretability is paramount, the PNGM approach allows one to reduce the dimensionality prior to differentiation. This structurally restricts the necessary reproductive value calculations to only the focal classes (Appendix C), thereby simplifying the stability conditions while retaining the biological intuition of the life cycle. By choosing between these algebraic and reductionist approaches, researchers can flexibly tackle the stability analysis of complex models.

The present framework is also applicable to ecological models, particularly for analyzing the spread of invasive species. For example, Hastings & Botsford (2006a,b) used analogous equations to investigate how spatial structure influences invasion dynamics. More recently, building on the target reproduction number developed by Lewis et al. (2019), Harrington et al. (2023) examined source-sink metapopulation dynamics in sea lice (Lepeophtheirus salmonis), a parasitic species threatening the salmon farming industry. The next-generation matrix approach has proven highly effective for evaluating persistence in metapopulations with well-characterized dispersal networks. In this context, the PNGM offers a mathematically grounded strategy to compress complex network structures into interpretable forms, enhancing both biological understanding and management decisions. However, this framework applies strictly when the invader is rare. Mathematically, the geometric series used to compute the PNGM must converge, which is guaranteed only when the spectral radius of the secondary sub-process is strictly less than unity. Once the species becomes widespread and density-dependent effects alter the transition rates, these initial approximations no longer hold, emphasizing the need for early detection in invasion management.

Having presented multiple fitness proxies that share the same invasion condition, a practical question arises: which method should one use? In practice, the invasion determinant and the PNGM serve complementary purposes. If the primary objective is algebraic manipulation or stability calculations (e.g., deriving selection gradients), the invasion determinant is often preferable. It yields a scalar criterion that can be differentiated systematically without requiring eigenvectors or an explicit partitioning of classes. Conversely, if the goal is biological interpretation, the PNGM is typically superior. It retains a clear life-cycle interpretation and preserves the reproductive-value weighting on the retained classes, explicitly clarifying which pathways contribute most to mutant success. The main practical challenge when using the PNGM is selecting the primary and secondary groups. We recommend defining the primary group based on the specific biological question (e.g., birth or key transmission events) and treating the intermediate classes as secondary. When multiple admissible partitions are available, one should select the partition that yields the most interpretable reduced proxy, as the fundamental invasion threshold remains invariant across all choices.

Finally, we outline the underlying ecological assumptions for applying this framework. First, we assume that the resident population dynamics are regulated by sufficient density dependence to reach a unique, strictly positive, and globally stable equilibrium. A standard local stability analysis is typically sufficient to ensure that the population does not depart from the resident equilibrium once established. Formally, ecological equilibria often change only slightly following recurrent gene substitutions (Geritz et al. 2002). While bistability or multiple attractors can complicate the analysis, such systems can generally be handled by analyzing the invasibility of mutants at each stable equilibrium separately.

Second, we assume that the transition matrix of the population model is irreducible (Stott et al. 2010). Biologically, this means that for any pair of distinct classes (k, m), there is at least one sequence of transitions from m to k. While seemingly restrictive, this assumption aligns naturally with the core premises of adaptive dynamics. In reducible models, gene flow between certain classes is permanently blocked, which contradicts the invasion-implies-substitution principle (Figure 3). For instance, if a system has a one-way transition from class 2 to class 3 with no return path (Figure 3A), a mutant arising in class 3 has zero chance of fixation regardless of its selective advantage. Similarly, a population perfectly split into two disconnected subgroups (Figure 3C) functions as two independent evolutionary entities and must be analyzed as such. Thus, the irreducibility assumption simply ensures that the population forms a single, cohesive evolutionary unit.

To conclude, we have unified the methodology of evolutionary invasion analysis for class-structured populations under the framework of structural evolutionary invasion analysis. By integrating the invasion determinant, the arbitrary decomposability of the next-generation matrix, and the projected next-generation matrix, we provide researchers with flexible tools that can

be used interchangeably or in combination. Furthermore, this framework naturally complements integral projection models, paving the way for the rigorous analysis of infinite-dimensional evolutionary demography.

References

Ajar, É. (2003). Analysis of disruptive selection in subdivided populations. *BMC Evol. Biol.*, **3**.1, p. 22. DOI: 10.1186/1471-2148-3-22.

Avila, P. & Mullon, C. (2023). Evolutionary game theory and the adaptive dynamics approach: adaptation where individuals interact. *Phil. Trans. R. Soc. B*, **378**.1876. DOI: 10.1098/rstb.2021.0502.

Berman, A. & Plemmons, R. J. (1987). *Nonnegative matrices in the mathematical sciences*. Classics in applied mathematics 9. Society for Industrial and Applied Mathematics.

Boots, M. & Best, A. (2018). The evolution of constitutive and induced defences to infectious disease. *Proc. R. Soc. B*, **285**.1883. DOI: 10.1098/rspb.2018.0658.

Buckingham, L. J., Bruns, E. L., & Ashby, B. (2023). The evolution of age-specific resistance to infectious disease. *Proc. R. Soc. B*, **290**.1991. DOI: 10.1098/rspb.2022.2000.

Bulmer, M. G. & Taylor, P. D. (1980). Dispersal and the sex ratio. *Nature*, **284**.5755, pp. 448–449. DOI: 10.1038/284448a0.

Caswell, H. (2001). *Matrix population models*. Wiley Online Library.

Charnov, E. L. (1976). Optimal foraging, the marginal value theorem. *Theor. Popul. Biol.*, **9**.2, pp. 129–136. DOI: 10.1016/0040-5809(76)90040-x.

Christiansen, F. B. (1991). On conditions for evolutionary stability for a continuously varying character. *Am. Nat.*, pp. 37–50. DOI: 10.1086/285203.

Coulson, T., Benton, T., Lundberg, P., Dall, S., Kendall, B., & Gaillard, J.-M. (2005). Estimating individual contributions to population growth: evolutionary fitness in ecological time. *Proc. R. Soc. B*, **273**.1586, pp. 547–55. DOI: 10.1098/rspb.2005.3357.

Courteau, J. & Lessard, S. (2000). Optimal sex ratios in structured populations. *J. Theor. Biol.*, **207**.2, pp. 159–175. DOI: 10.1006/jtbi.2000.2160.

Cushing, J. M. (1998). *An Introduction to Structured Population Dynamics*. Society for Industrial and Applied Mathematics. DOI: 10.1137/1.9781611970005.

Day, T. & Burns, J. G. (2003). A consideration of patterns of virulence arising from host-parasite coevolution. *Evolution*, **57**.3, pp. 671–676. DOI: 10.1111/j.0014-3820.2003.tb01558.x.

de Camino Beck, T. & Lewis, M. A. (2007). A new method for calculating net reproductive rate from graph reduction with applications to the control of invasive species. *Bull. Math. Biol.*, **69**.4, pp. 1341–1354. DOI: 10.1007/s11538-006-9162-0.

Dieckmann, U. & Law, R. (1996). The dynamical theory of coevolution: a derivation from stochastic ecological processes. *J. Math. Biol.*, **34**.5-6, pp. 579–612. DOI: 10.1007/s002850050022.

Diekmann, O., Heesterbeek, J. A. P., & Metz, J. A. J. (1990). On the definition and the computation of the basic reproduction ratio R_0 in models for infectious diseases in heterogeneous populations. *J. Math. Biol.*, **28**.4. DOI: 10.1007/bf00178324.

Easterling, M. R., Ellner, S. P., & Dixon, P. M. (2000). Size-specific sensitivity: applying a new structured population model. *Ecology*, **81**.3, pp. 694–708. DOI: 10.1890/0012-9658(2000)081[0694:sssaan]2.0.co;2.

Ellner, S. P., Childs, D. Z., & Rees, M. (2016). *Data-driven modelling of structured populations*. Springer.

Eshel, I. (1996). On the changing concept of evolutionary population stability as a reflection of a changing point of view in the quantitative theory of evolution. *J. Math. Biol.*, **34**.5–6, pp. 485–510. DOI: 10.1007/bf02409747.

Ewens, W. J. (2004). *Mathematical Population Genetics: I. Theoretical Introduction*. 2nd ed. Interdisciplinary Applied Mathematics 27. Springer-Verlag New York.

Fisher, R. A. (1930). *The genetical theory of natural selection*. Clarendon Press. DOI: 10.5962/bhl.title.27468.

— (1941). Average excess and average effect of a gene substitution. *Ann. Eugen.*, **11**.1, pp. 53–63. DOI: 10.1111/j.1469-1809.1941.tb02272.x.

Frank, S. A. (1998). *Foundations of social evolution*. Princeton University Press.

— (1987). Demography and sex ratio in social spiders. *Evolution*, **41**.6, pp. 1267–1281. DOI: 10.1111/j.1558-5646.1987.tb02465.x.

Geritz, S. A. H., Kisdi, É., Meszéna, G., & Metz, J. (1998). Evolutionarily singular strategies and the adaptive growth and branching of the evolutionary tree. *Evol. Ecol.*, **12**.1, pp. 35–57. DOI: 10.1023/a:1006554906681.

Geritz, S. A. H. (2005). Resident-invader dynamics and the coexistence of similar strategies. *J. Math. Biol.*, **50**.1, pp. 67–82. DOI: 10.1007/s00285-004-0280-8.

Geritz, S. A. H., Gyllenberg, M., Jacobs, F. J., & Parvinen, K. (2002). Invasion dynamics and attractor inheritance. *J. Math. Biol.*, **44**.6, pp. 548–560. DOI: 10.1007/s002850100136.

Guillaume, F. & Otto, S. P. (2012). Gene functional trade-offs and the evolution of pleiotropy. *Genetics*, **192**.4, pp. 1389–1409. DOI: 10.1534/genetics.112.143214.

Hamilton, W. D. (1967). Extraordinary sex ratios. *Science*, **156**.3774, pp. 477–488. DOI: 10.1126/science.156.3774.477.

Hamilton, W. D. & May, R. M. (1977). Dispersal in stable habitats. *Nature*, **269**.5629, pp. 578–581. DOI: 10.1038/269578a0.

Harrington, P. D., Cantrell, D. L., & Lewis, M. A. (2023). Next-generation matrices for marine metapopulations: The case of sea lice on salmon farms. *Ecol. Evol.*, **13**.4. DOI: 10.1002/ece3.10027.

Hastings, A. & Botsford, L. W. (2006a). A simple persistence condition for structured populations. *Ecol. Lett.*, **9**.7, pp. 846–852. DOI: 10.1111/j.1461-0248.2006.00940.x.

— (2006b). Persistence of spatial populations depends on returning home. *Proc. Natl. Acad. Sci. USA*, **103**.15, pp. 6067–6072. DOI: 10.1073/pnas.0506651103.

Hofbauer, J. & Sigmund, K. (1990). Adaptive dynamics and evolutionary stability. *Appl. Math. Lett.*, **3**.4, pp. 75–79. DOI: 10.1016/0893-9659(90)90051-c.

Hurford, A., Cownden, D., & Day, T. (2010). Next-generation tools for evolutionary invasion analyses. *J. R. Soc. Interface*, **7**.45, pp. 561–571. DOI: 10.1098/rsif.2009.0448.

Inaba, H. & Nishiura, H. (2008). The state-reproduction number for a multistate class age structured epidemic system and its application to the asymptomatic transmission model. *Math. Biosci.*, **216**.1, pp. 77–89. DOI: 10.1016/j.mbs.2008.08.005.

Iritani, R. & Cheptou, P.-O. (2017). Joint evolution of differential seed dispersal and self-fertilization. *J. Evol. Biol.*, **30**.8, pp. 1526–1543. DOI: 10.1111/jeb.13120.

Iritani, R. (2020). Gametophytic competition games among relatives: when does spatial structure select for facilitativeness or competitiveness in pollination? *J. Ecol.*, **108**.1, pp. 1–13. DOI: 10.1111/1365-2745.13282.

Iritani, R. & Iwasa, Y. (2014). Parasite infection drives the evolution of state-dependent dispersal of the host. *Theor. Popul. Biol.*, **92**, pp. 1–13. DOI: 10.1016/j.tpb.2013.10.005.

Iritani, R., Visher, E., & Boots, M. (2019). The evolution of stage-specific virulence: Differential selection of parasites in juveniles. *Evol. Lett.*, **3**.2, pp. 162–172. DOI: 10.1002/evl3.105.

Iritani, R., West, S. A., & Abe, J. (2021). Cooperative interactions among females can lead to even more extraordinary sex ratios. *Evol. Lett.*, **5**.4, pp. 370–384. DOI: 10.1002/evl3.217.

Kemeny, J. G., Snell, J., & Knapp, A. (1966). *Markov chains*. New York, NY: University Series in Higher Mathematics, Van Nostrand.

Kruuk, L. & Hill, W. (2008). Evolutionary dynamics of wild populations: the use of long-term pedigree data. *Proc. R. Soc. B*, **275**.1635, pp. 593–596. DOI: 10.1098/rspb.2007.1689.

Kuijper, B. & Johnstone, R. A. (2019). The evolution of early-life effects on social behaviour—why should social adversity carry over to the future? *Phil. Trans. R. Soc. B*, **374**.1770, p. 20180111. DOI: 10.1098/rstb.2018.0111.

Lande, R. & Schemske, D. W. (1985). The evolution of self-fertilization and inbreeding depression in plants. I. Genetic models. *Evolution*, **39**.1, pp. 24–40. DOI: 10.1111/j.1558-5646.1985.tb04077.x.

Lefkovitch, L. P. (1965). The study of population growth in organisms grouped by stages. *Biometrics*, **21**.1, p. 1. DOI: 10.2307/2528348.

Lewis, M. A., Shuai, Z., & van den Driessche, P. (2019). A general theory for target reproduction numbers with applications to ecology and epidemiology. *J. Math. Biol.*, DOI: 10.1007/s00285-019-01345-4.

Li, C.-K. & Schneider, H. (2002). Applications of Perron-Frobenius theory to population dynamics. *J. Math. Biol.*, **44**.5, pp. 450–462. DOI: 10.1007/s002850100132.

Lion, S. & Metz, J. A. J. J. (2018). Beyond R_0 maximisation: on pathogen evolution and environmental dimensions. *Trends Ecol. Evol.*, **33**, pp. 75–90. DOI: 10.1016/j.tree.2018.02.004.

Massol, F., Calcagno, V., & Massol, J. (2009). The metapopulation fitness criterion: Proof and perspectives. *Theor. Popul. Biol.*, **75**.2–3, pp. 183–200. DOI: http://dx.doi.org/10.1016/j.tpb.2009.02.005.

Massol, F. & Débarre, F. (2015). Evolution of dispersal in spatially and temporally variable environments: The importance of life cycles. *Evolution*, **69**.7, pp. 1925–1937. DOI: 10.1111/evo.12699.

Maynard Smith, J. (1982). *Evolution and the Theory of Games*. Cambridge university press.

Maynard Smith, J. & Price, G. R. (1973). The logic of animal conflict. *Nature*, **246**, p. 15. DOI: 10.1038/246015a0.

Metz, J. A. J. & Leimar, O. (2011). A simple fitness proxy for structured populations with continuous traits, with case studies on the evolution of haplo-diploids and genetic dimorphisms. *J. Biol. Dynam.*, **5**.2, pp. 163–190. DOI: 10.1080/17513758.2010.502256.

Metz, J. A. & Gyllenberg, M. (2001). How should we define fitness in structured metapopulation models? Including an application to the calculation of evolutionarily stable dispersal strategies. *Proc. R. Soc. B*, **268**.1466, pp. 499–508.

Metz, J. A., Nisbet, R., & Geritz, S. (1992). How should we define 'fitness' for general ecological scenarios? *Trends Ecol. Evol.*, **7**.6, pp. 198–202.

Mitchell, E., Graham, A. L., Úbeda, F., & Wild, G. (2022). On maternity and the stronger immune response in women. *Nat. Commun.*, **13**.1. DOI: 10.1038/s41467-022-32569-6.

Mullon, C., Keller, L., & Lehmann, L. (2016). Evolutionary stability of jointly evolving traits in subdivided populations. *Am. Nat.*, **188**.2, pp. 175–195. DOI: 10.1086/686900.

Mullon, C. & Lehmann, L. (2014). The robustness of the weak selection approximation for the evolution of altruism against strong selection. *J. Evol. Biol.*, **27**.10, pp. 2272–2282. DOI: 10.1111/jeb.12462.

Pelletier, F., Clutton-Brock, T., Pemberton, J., Tuljapurkar, S., & Coulson, T. (2007). The Evolutionary Demography of Ecological Change: Linking Trait Variation and Population Growth. *Science*, **315**.5818, pp. 1571–1574. DOI: 10.1126/science.1139024.

Priklopil, T. & Lehmann, L. (2020). Invasion implies substitution in ecological communities with class-structured populations. *Theor. Popul. Biol.*, **134**, pp. 36–52. DOI: 10.1016/j.tpb.2020.04.004.

— (2024). On the interpretation of the operation of natural selection in class-structured populations. *Am. Nat.*, **203**.2, pp. 292–304. DOI: 10.1086/727970.

Rees, M. & Ellner, S. P. (2016). Evolving integral projection models: evolutionary demography meets eco-evolutionary dynamics. *Methods Ecol. Evol.*, **7**.2, pp. 157–170. DOI: 10.1111/2041-210x.12487.

Roberts, M. G. & Heesterbeek, J. A. P. (2003). A new method for estimating the effort required to control an infectious disease. *Proc. R. Soc. B*, **270**.1522, pp. 1359–1364. DOI: 10.1098/rspb.2003.2339.

Rodrigues, A. M. M. & Gardner, A. (2015). Simultaneous failure of two sex-allocation invariants: implications for sex-ratio variation within and between populations. *Proc. R. Soc. B*, **282**.1810, p. 20150570. DOI: 10.1098/rspb.2015.0570.

Rodrigues, A. M. M. & Gardner, A. (2012). Evolution of helping and harming in heterogeneous populations. *Evolution*, **66**.7, pp. 2065–2079. DOI: 10.1111/j.1558-5646.2012.01594.x.

— (2013). Evolution of helping and harming in heterogeneous groups. *Evolution*, **67**.8, pp. 2284–2298. DOI: 10.1111/j.1558-5646.2012.01594.x.

Rousset, F. (2004). *Genetic Structure and Selection in Subdivided Populations (MPB-40)*. Princeton University Press.

Rueffler, C. & Metz, J. A. J. (2013). Necessary and sufficient conditions for R_0 to be a sum of contributions of fertility loops. *J. Math. Biol.*, **66**.4-5, pp. 1099–1122. DOI: 10.1007/s00285-012-0575-0.

Rueffler, C., Metz, J. A. J., & Van Dooren, T. J. M. (2012). What life cycle graphs can tell about the evolution of life histories. *J. Math. Biol.*, **66**.1-2, pp. 225–279. DOI: 10.1007/s00285-012-0509-x.

Stott, I., Townley, S., Carslake, D., & Hodgson, D. J. (2010). On reducibility and ergodicity of population projection matrix models. *Methods Ecol. Evol.*, **1**.3, pp. 242–252. DOI: 10.1111/j.2041-210x.2010.00032.x.

Takada, T. & Kigami, J. (1991). The dynamical attainability of ESS in evolutionary games. *J. Math. Biol.*, **29**.6, pp. 513–529. DOI: 10.1007/bf00164049.

Takada, T. & Nakajima, H. (1992). An analysis of life history evolution in terms of the density-dependent Lefkovitch matrix model. *Math. Biosci.*, **112**.1, pp. 155–176. DOI: 10.1016/0025-5564(92)90091-a.

— (1998). Theorems on the invasion process in stage-structured populations with density-dependent dynamics. *J. Math. Biol.*, **36**.5, pp. 497–514. DOI: 10.1007/s002850050111.

Taylor, P. D. (1988). An inclusive fitness model for dispersal of offspring. *J. Theor. Biol.*, **130**.3, pp. 363–378. DOI: 10.1016/s0022-5193(88)80035-3.

— (1990). Allele-frequency change in a class-structured population. *Am. Nat.*, **135**, pp. 95–106. DOI: 10.1086/285034.

— (1992). Altruism in viscous populations—an inclusive fitness model. *Evol. Ecol.*, **6**.4, pp. 352–356. DOI: 10.1007/bf02270971.

Taylor, P. D. & Bulmer, M. G. (1980). Local mate competition and the sex ratio. *J. Theor. Biol.*, **86**.3, pp. 409–419. DOI: 10.1016/0022-5193(80)90342-2.

Tuljapurkar, S., Horvitz, C. C., & Pascarella, J. B. (2003). The many growth rates and elasticities of populations in eandom environments. *Am. Nat.*, **162**.4, pp. 489–502. DOI: 10.1086/378648.

Úbeda, F. & Jansen, V. A. A. (2016). The evolution of sex-specific virulence in infectious diseases. *Nat. Commun.*, **7**, p. 13849. DOI: 10.1038/ncomms13849.

van den Driessche, P. & Watmough, J. (2002). Reproduction numbers and sub-threshold endemic equilibria for compartmental models of disease transmission. *Math. Biosci.*, **180**.1, pp. 29–48. DOI: 10.1016/s0025-5564(02)00108-6.

Wright, S. (1931). Evolution in Mendelian populations. *Genetics*, **16**.2, p. 97. DOI: 10.1007/bf02459575.

Box 1: Classifying NGMs based on the invasion threshold

In the main text, we have seen that some NGMs have the same invasion condition. It is therefore useful to classify typical formulas of the NGMs with shared invasion threshold. In this box, we say that two NGMs G_1 and G_2 are invadability-equivalent if $\rho(G_1) \gtreqless 1 \Leftrightarrow \rho(G_2) \gtreqless 1$.

In Appendix C, we show that the following NGMs are invadability-equivalent, whenever F and S are both nonnegative regardless of their actual biological meanings: $F+S, (I-S)^{-1}F, F(I-S)^{-1}$ and $\left(\begin{smallmatrix} F & S \\ F & S \end{smallmatrix}\right)$ (Box-Fig 1). The last NGM has twice as large size as the original, and may be practically relevant when the class transition is unbiased (Rueffler *et al.* 2012; Lion & Metz 2018; Iritani *et al.* 2019, also see Example 2). We duplicated the focal class into two replicas with the same reproductive value. The life-cycle graph is expanded by creating a replica of the duplicated classes.

Whenever the inversion exists and F and S are nonnegative, these NGMs are invadability-equivalent to each other. This result is therefore a simple generalization of the so-called 'fundamental matrix' in population demography (Cushing 1998; Li & Schneider 2002).

One may wonder which NGM to use. One may preferably use the 'snapshot' fitness $F+S$ for its numerical stability over the others involving matrix inversions. From an algebraic perspective, determining the stability properties of evolutionary equilibrium involves partial derivatives; again, the snapshot form ($F+S$) may seem preferable, but at the cost of higher dimensionality than the inverse formulas such as $F(I-S)^{-1}$ if F contains many zeros or redundancies (said to be 'rank deficient' in linear algebra).

$$G = F+S; \qquad (I-S)^{-1}F = F+SF+S^2F+\cdots; \qquad F(I-S)^{-1} = F+FS+FS^2+\cdots; \qquad \left(\begin{array}{c|c} F & S \\ \hline F & S \end{array}\right);$$

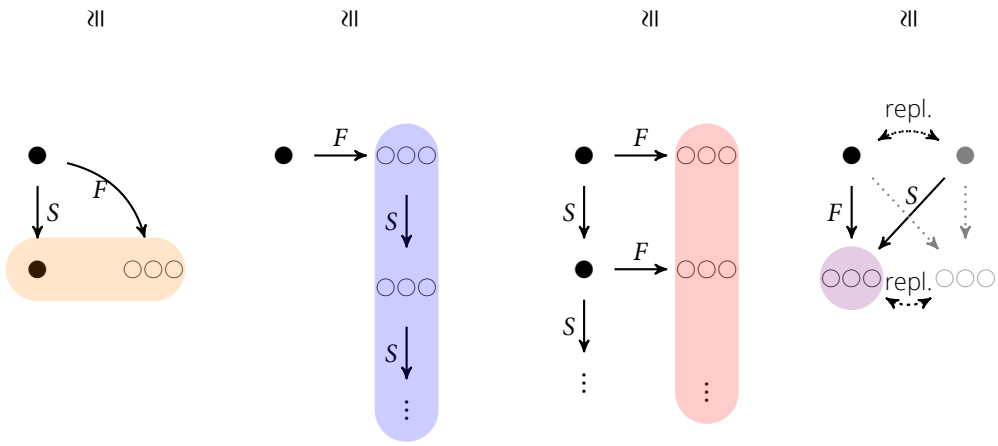

Box-Fig 1:The invadability-equivalent NGMs (top) and the corresponding structures of NGMs (bottom). The colors correspond to the highlighted terms in the equation. Closed circle: focal individual; open cicles: offspring of focal individual; Gray circle: focal-individual replica. Gray pathway should not be counted in to avoid the double-counting of fitness. "repl." for mirroerd replica.

Box 2: Calculation techniques

In practice, the invasion condition may involve fractional terms such as $w := \phi(z+\delta, z)/\mu(z+\delta, z)$, where z is resident phenotype, with δ small. The derivative has a useful formula:

$$\frac{1}{w} \cdot \frac{\partial w}{\partial \delta} = \left(\frac{\phi^{(1)}}{\phi} - \frac{\mu^{(1)}}{\mu} \right),$$

where $^{(1)}$ represents the first derivative with respect to δ. This is a form of the marginal value theorem linking the trade-off relationship between the marginal increases in the numerator (typically, fecundity) and the denominator (typically, mortality) (Charnov 1976). In population genetics, this expression is called as the average excess of gene substitution (Fisher 1941).

Invasion conditions often contain the cumulative survival probability terms like $s' := \prod_k s'_k$ where s'_k represents a survival or transition probability from class k and $\prod_k$ represents the product operator over k. Its derivative also has a useful formula:

$$\frac{1}{s} \cdot \frac{\partial s}{\partial \delta} = \sum_k \frac{s_k^{(1)}}{s_k}.$$

This expression can be also viewed as selection leading to the balanced, marginal increases in survival probabilities.

The common technique behind these derivatives is logarithmic differentiation to compute marginal changes in reproductive success. The following, matrix-analogue of the logarithmic derivative of the sojourn time is also useful:

$$\frac{\partial}{\partial \delta} (I - S)^{-1} = (I - S)^{-1} S^{(1)} (I - S)^{-1}. \tag{12}$$

The matrix $(I - S)^{-1}$, called as the fundamental matrix (Kemeny *et al.* 1966), represents the expected number of visits to a class starting from another class.

A note on interpretability: while symbolic computation software is powerful, automated simplification often obscures biological insight by expanding meaningful compound terms (e.g., life-history trade-offs). Differentiation should be viewed not merely as an algebraic operation but as a mapping that preserves the biological structure of fitness. Therefore, we recommend rearranging the derived equations to maintain biological interpretability, and prioritizing meaningful groupings over mathematical brevity.

Box 3: Properties of the structural evolutionary invasion analysis

Timescale separation First, we obtain the PNGM as a result of separation of timescales between primary (which we assume is slow) and secondary (fast) groups. Biologically, this means that we can focus on only an arbitrary subset of classes to capture the overall gene-frequency changes (Appendix C). Note that one does not need any a priori knowledge or assumption of the actual differences in timescales of the classes. The utility of this method is clearly illustrated in the dispersal model (Example 3), where the class is defined as the number of mutant in a patch and the timescale is separated based on the purpose of deriving fitness, regardless of biological assumption on the timescales.

Fisher's reproductive values Second, Fisher's (1930) reproductive values of the primary group do not change with PNGM (Appendix C). This property reflects the reproductive values' nature of measuring the asymptotically long-term contributions to the gene pool (Taylor 1990; Caswell 2001; Rousset 2004). Note that more precisely, the invariance in the reproductive values hold only for neutral mutants (first order effect; Taylor 1990) but not for selectively non-neutral mutants.

Inheriting stability characteristics Practically, the ultimate goal of applying the adaptive dynamics framework is to locate and characterize evolutionary equilibrium (EE), namely the direction of selection and possibility of disruptive selection. These characteristics of EE can be analyzed through:

(i) the first derivative of invasion fitness (i.e., selection gradient capturing the location of EE);

(ii) how the direction of selection changes with the resident trait value (i.e., convergence stability or attainability); and

(iii) the second derivative of invasion fitness (i.e., whether selection is disruptive or stabilizing around EE; Maynard Smith & Price 1973; Maynard Smith 1982; Christiansen 1991; Takada & Kigami 1991; Eshel 1996).

Regardless of using the original NGM, invasion determinant, or PNGM, the resulting invasion conditions give the same stability properties (i)–(iii). Thus, one can characterize both the location and stability of EE using the structural evolutionary invasion analysis. See Appendix D for details.

APPENDIX

A Invasion determinant formula

Resident NGM

We here show that the resident NGM has a unity spectral radius. This result is obvious for discrete-time models. We thus derive the result for continuous-time models.

To see this, consider two types each with density $\vec{N}$ and $\vec{N'}$. Ignoring mutation, we can describe their dynamics as:

$$\begin{aligned} \frac{\mathrm{d}\vec{N}}{\mathrm{d}t} &= A(z \mid E)\vec{N}, \\ \frac{\mathrm{d}\vec{N'}}{\mathrm{d}t} &= A(z' \mid E)\vec{N'}, \end{aligned} \tag{A-1}$$

where $E = \left(\vec{N}, \vec{N'}, z, z'\right)$. Note that these are generally nonlinear because of E.

At the resident equilibrium with no mutant,

$$A(z \mid E^\circ)\vec{N^\circ} = \vec{0}, \quad E^\circ = \left(\vec{N^\circ}, \vec{0}, z, z\right). \tag{A-2}$$

When the mutant is rare, its dynamics can be linearized as:

$$\frac{\mathrm{d}\vec{N'}}{\mathrm{d}t} = A(z' \mid E^\circ)\vec{N'} = J(z' \mid E^\circ)\vec{N'}. \tag{A-3}$$

Thus, the Jacobian matrix evaluated at the resident equilibrium is exactly $J(z' \mid E^\circ) = A(z' \mid E^\circ)$.

At neutrality ($z' = z$), substituting this into the resident equilibrium condition yields:

$$J^\circ\vec{N^\circ} = \vec{0}, \tag{A-4}$$

where $J^\circ \coloneqq J(z \mid E^\circ)$.

Decomposing the Jacobian as $J^\circ = U^\circ - V^\circ$ according to the NGM framework, we get:

$$(U^\circ - V^\circ)\vec{N^\circ} = \vec{0} \implies U^\circ\vec{N^\circ} = V^\circ\vec{N^\circ}. \tag{A-5}$$

Since the neutral NGM is defined as $G^\circ = U^\circ (V^\circ)^{-1}$, we get:

$$G^\circ\left(V^\circ\vec{N^\circ}\right) = V^\circ\vec{N^\circ}. \tag{A-6}$$

Because the matrix U° is non-negative and the equilibrium density $\vec{N^\circ}$ is strictly positive, the vector $U^\circ\vec{N^\circ}$ must be non-negative and non-zero. The equation $G^\circ U^\circ\vec{N^\circ} = U^\circ\vec{N^\circ}$ indicates that $U^\circ\vec{N^\circ}$ is an eigenvector of G° associated with the unit eigenvalue. By the Perron-Frobenius theorem for non-negative irreducible matrices, an eigenvalue associated with a non-negative eigenvector must be the spectral radius. Therefore, $\rho(G^\circ) = 1$.

Theorem on the invasion determinant

We here prove the invasion determinant.

Theorem 1 (Invasion determinant formula)**.** Let G be a next-generation matrix, and assume that the selection is weak. Then,

$$\rho(G) \gtreqless 1 \iff -\det(I - G) \gtreqless 0. \tag{A-7}$$

Proof. Let $\Gamma_M(x) \coloneqq \det(xI - M)$ be the monic characteristic polynomial of a matrix M, and G° be the mutant NGM G evaluated at $\delta = 0$ (i.e., the neutral mutant matrix). Thus, we have $\rho(G^\circ) = 1$ and so, by continuity of the spectrum of G, we have $\rho(G) = \rho(G^\circ) + \varepsilon = 1 + \varepsilon$ where ε is small. Furthermore, the Perron-Frobenius theorem for irreducible nonnegative matrix implies that the spectral radius of G is a simple eigenvalue of G and so $\Gamma_G(\rho(G)) = 0$ and $\mathrm{d}\Gamma_G(x)/\,\mathrm{d}x|_{x=\rho(G)} > 0$. As a result, if δ is small we can expand the equation $\Gamma_G(1+\varepsilon) = 0$ in powers of ε to obtain $\Gamma_G(1) + \mathrm{d}\Gamma_G(x)/\,\mathrm{d}x|_{x=\rho(G)}\varepsilon + o(\varepsilon) = 0$. Given $\varepsilon = \rho(G) - 1$, for small enough δ and thus ε this can be re-written as $\mathrm{sign}(\rho(G) - 1) = \mathrm{sign}(-\Gamma_G(1))$. Finally, from the definition of $\Gamma_G(x)$ this can be re-written as $\mathrm{sign}(\rho(G) - 1) = \mathrm{sign}(-\det(I - G))$ from which the theorem follows. □

The corresponding result for the original continuous-time Jacobian reads:

$$\rho(G) \gtreqless 1 \quad \Leftrightarrow \quad -\det(-J) \gtreqless 0. \tag{A-8}$$

To prove this we decompose $J = U - V$ into the components that satisfy the hypotheses of NGM. With some rearrangement, we get:

$$\det(-J) = \det(V - U) = \det(I - G)\det(V). \tag{A-9}$$

We notice that V has nonnpositive elements at off-diagonal components while positive element at diagonal components, and V^{-1} is nonnegative. We can thus, using the theory of M-matrix, we have $\det(V) > 0$ (Berman & Plemmons 1987). Therefore, $\det(-J)$ and $\det(I - G)$ have the same sign, and thus both can be used for invasion condition.

B Nonnegative decomposition theorem

We here show that any NGM can be split into nonnegative and nonzero matrices and converted to an alternative.

Theorem 2 (Nonnegative decomposition theorem)**.** Let G be a (irreducible) next-generation matrix, and assume that the selection is weak. Put $G = H_1 + H_2$ where H_1 and H_2 are both nonnegative and nonzero for values of δ within some neighbourhood of $\delta = 0$. Then,

1. for small enough δ, the matrix $I - H_2$ is invertible and thus $\widehat{G} \coloneqq H_1\,(I - H_2)^{-1}$ is well-defined, and
2. if $\widehat{G}$ is irreducible, the following equivalency holds:

$$\rho(G) \gtreqless 1 \Longleftrightarrow \rho\left(\widehat{G}\right) \gtreqless 1. \tag{B-1}$$

Proof. We first show that $I - H_2$ is invertible whenever H_1 is nonzero. For this, we use Corollary 2.1.5 of Berman & Plemmons (1987, p. 27), which is stated as follows:

Lemma 1 (Berman and Plemmons 1994)**.** Let A and B be nonnegative matrices. If $B - A$ is nonnegative with $B - A \neq O$, and if $A + B$ is irreducible, then $\rho(A) < \rho(B)$.

We take $A = H_2^\circ$ and $B = G^\circ$. We have $B - A = H_1^\circ$, which is nonnegative and nonzero by our assumption. Furthermore, because $B = G^\circ$ is irreducible by the standard assumption of the NGM, and $O \leq A \leq B$, the sum $A + B$ shares the exact same zero-nonzero pattern as B, making $A + B$ irreducible as well. Thus, the hypotheses of Lemma 1 are satisfied, yielding $\rho(H_2^\circ) < \rho(G^\circ) = 1$. By the continuity of the spectral radius with respect to matrix entries, $\rho(H_2)$ is continuous in δ. Therefore, $\rho(H_2) < 1$ under weak selection (i.e., for small enough $|\delta|$), which implies that $I - H_2$ is invertible and completes the proof of the first statement.

To prove the second part, we use the invasion determinant. By definition of $\widehat{G} = H_1\,(I - H_2)^{-1}$, we have:

$$-\det\left(I - \widehat{G}\right) = \frac{-\det(I - H_1 - H_2)}{\det(I - H_2)} = \frac{-\det(I - G)}{\det(I - H_2)}. \tag{B-2}$$

Because $\rho(H_2) < 1$ and H_2 is nonnegative, the monic characteristic polynomial of H_2 is positive at unity, so $\Gamma_{H_2}(1) = \det(I - H_2) > 0$. Therefore, $-\det\left(I - \widehat{G}\right)$ and $-\det(I - G)$ share the exact same sign.

Because G is irreducible, Theorem 1 guarantees that $\rho(G) \gtreqless 1 \iff -\det(I - G) \gtreqless 0$. Likewise, because the reduced matrix $\widehat{G}$ is explicitly assumed to be irreducible in the theorem statement, applying Theorem 1 to $\widehat{G}$ yields $-\det\left(I - \widehat{G}\right) \gtreqless 0 \iff \rho\left(\widehat{G}\right) \gtreqless 1$. Connecting these equivalences through the shared sign of their determinants completes the proof. □

The nonnegative decomposition theorem is based on a matrix splitting method known as 'regular splitting' for numerical analysis (Varga 1963).

C PNGM

Derivation of PNGM

We here prove the following theorem.

Theorem 3 (Projected Next-Generation Theorem)**.** Let G be a next-generation matrix of a mutant, with the following block-partition structure:

$$G = \left(\begin{array}{c:c} G_{\mathbb{X},\mathbb{X}} & G_{\mathbb{X},\mathbb{Y}} \\ \hdashline G_{\mathbb{Y},\mathbb{X}} & G_{\mathbb{Y},\mathbb{Y}} \end{array}\right). \tag{C-1}$$

Then, under weak selection, the following results hold true:

1. $\rho\left(G_{\mathbb{Y},\mathbb{Y}}\right) < 1$.
2. $$\rho(G) \gtreqless 1 \quad \iff \quad \rho(\mathcal{R}_{\mathbb{X}}(G)) \gtreqless 1, \tag{C-2}$$

   where
   $$\mathcal{R}_{\mathbb{X}}(G) \coloneqq G_{\mathbb{X},\mathbb{X}} + G_{\mathbb{X},\mathbb{Y}}\left(I - G_{\mathbb{Y},\mathbb{Y}}\right)^{-1} G_{\mathbb{Y},\mathbb{X}}. \tag{C-3}$$

The first part can be proved in the same way as the first part of Theorem 1. The second part is also a direct implication of Theorem 2: choose the decomposition as $H_1 \coloneqq \Pi_{\mathbb{X}} G$ with $H_2 = G - H_1 = \Pi_{\mathbb{Y}} G$, where $\Pi_{\mathbb{X}}$ and $\Pi_{\mathbb{Y}}$ are projection matrices (Roberts & Heesterbeek 2003); note that a matrix Π is called as projection if $\Pi^2 = \Pi$.

We here provide a similar, alternative proof. Specifically, we use the Schur complement and Schur's determinant identity (Crabtree & Haynsworth 1969).

Definition 1 (Schur complement)**.** Let M be a square matrix block-partitioned as:

$$M = \left(\begin{array}{c:c} M_{\mathbb{X},\mathbb{X}} & M_{\mathbb{X},\mathbb{Y}} \\ \hdashline M_{\mathbb{Y},\mathbb{X}} & M_{\mathbb{Y},\mathbb{Y}} \end{array}\right) \tag{C-4}$$

Suppose $M_{\mathbb{Y},\mathbb{Y}}$ is invertible. We define the Schur complement of M to $M_{\mathbb{Y},\mathbb{Y}}$, denoted by $\mathcal{S}_{\mathbb{X}}(M)$, as

$$\mathcal{S}_{\mathbb{X}}(M) \coloneqq M_{\mathbb{X},\mathbb{X}} - M_{\mathbb{X},\mathbb{Y}} M_{\mathbb{Y},\mathbb{Y}}^{-1} M_{\mathbb{Y},\mathbb{X}}. \tag{C-5}$$

By definition, $\mathcal{R}_{\mathbb{X}}(M) = I - \mathcal{S}_{\mathbb{X}}(I - M)$.

Lemma 2 (Schur)**.** Let M be a square matrix satisfying the assumptions of Definition 1. Then, the following identity holds true:

$$\det(\mathcal{S}_{\mathbb{X}}(M)) = \frac{\det(M)}{\det\left(M_{\mathbb{Y},\mathbb{Y}}\right)}. \tag{C-6}$$

(Proof of Lemma 2). Consider the identity:

$$\begin{pmatrix} M_{\mathbb{X},\mathbb{X}} & M_{\mathbb{X},\mathbb{Y}} \\ M_{\mathbb{Y},\mathbb{X}} & M_{\mathbb{Y},\mathbb{Y}} \end{pmatrix} \begin{pmatrix} I & O \\ -M_{\mathbb{Y},\mathbb{Y}}^{-1} M_{\mathbb{Y},\mathbb{X}} & I \end{pmatrix} = \begin{pmatrix} \mathcal{S}_{\mathbb{X}}(M) & M_{\mathbb{X},\mathbb{Y}} \\ O & M_{\mathbb{Y},\mathbb{Y}} \end{pmatrix}, \tag{C-7}$$

taking the determinant of which yields:

$$\det(M) \cdot 1 = \det(\mathcal{S}_{\mathbb{X}}(M)) \cdot \det\left(M_{\mathbb{Y},\mathbb{Y}}\right), \tag{C-8}$$

which yields the desired result. □

(Proof of Theorem 3). In Lemma 2, put $M = I - G$. By definition, we have:

$$\mathcal{S}_{\mathbb{X}}(M) = I - \mathcal{R}_{\mathbb{X}}(G) = I - G_{\mathbb{X},\mathbb{X}} - G_{\mathbb{X},\mathbb{Y}} \left(I - G_{\mathbb{Y},\mathbb{Y}}\right)^{-1} G_{\mathbb{Y},\mathbb{X}}. \tag{C-9}$$

Applying Lemma 2, we have:

$$\det(I - \mathcal{R}_{\mathbb{X}}(G)) = \frac{\det(I - G)}{\det\left(I - G_{\mathbb{Y},\mathbb{Y}}\right)}. \tag{C-10}$$

Because $\rho\left(G_{\mathbb{Y},\mathbb{Y}}\right) < 1$, the characteristic polynomial of $G_{\mathbb{Y},\mathbb{Y}}$ must be positive at unity, implying $\det\left(I - G_{\mathbb{Y},\mathbb{Y}}\right) > 0$. Hence the LHS and the numerator of the RHS have the same sign. This completes the proof. □

Interpretation of PNGM

We consider a mutant individual residing in one of the primary group classes and assess how many offspring it produces to the primary group. Specifically, we write P_n for a matrix of the total expected number of the mutant's offspring produced to the primary group over n subsequent generations. We then get:

$$\begin{aligned} P_n &= G_{\mathbb{X},\mathbb{X}} + G_{\mathbb{X},\mathbb{Y}} G_{\mathbb{Y},\mathbb{X}} + G_{\mathbb{X},\mathbb{Y}} G_{\mathbb{Y},\mathbb{Y}} G_{\mathbb{Y},\mathbb{X}} + \cdots + G_{\mathbb{X},\mathbb{Y}} (G_{\mathbb{Y},\mathbb{Y}})^{n-2} G_{\mathbb{Y},\mathbb{X}} \\ &= G_{\mathbb{X},\mathbb{X}} + \sum_{i=0}^{n-2} G_{\mathbb{X},\mathbb{Y}} (G_{\mathbb{Y},\mathbb{Y}})^i G_{\mathbb{Y},\mathbb{X}} \\ &= G_{\mathbb{X},\mathbb{X}} + G_{\mathbb{X},\mathbb{Y}} \left(I - (G_{\mathbb{Y},\mathbb{Y}})^{n-1}\right) \left(I - G_{\mathbb{Y},\mathbb{Y}}\right)^{-1} G_{\mathbb{Y},\mathbb{X}} \end{aligned} \tag{C-11}$$

where the first term represents the number of primary group-offspring directly produced by the mutant in one generation; the second term represents the number of primary group-grand-offspring whose parents are in the secondary group (the remaining terms can be read analogously). Because $\rho\left(G_{\mathbb{Y},\mathbb{Y}}\right) < 1$, we have $\lim_{n\to\infty} P_n = \mathcal{R}_{\mathbb{X}}(G)$ (Horn & Johnson 1985, Theorem 5.6.12). Hence, the PNGM counts the total number of offspring in the primary classes produced by the mutant from the primary classes throughout the lifespan.

Embedding of PNGM

Here we examine the relation between PNGM and nonnegative decomposition theorem. We specifically consider embedding $G = H_1 + H_2$ into a high dimensional space as:

$$\widetilde{G} := \begin{pmatrix} O & I \\ H_1 & H_2 \end{pmatrix}, \tag{C-12}$$

with:

$$\begin{aligned} \mathcal{R}_{\mathbb{X}}\left(\widetilde{G}\right) &= (I - H_2)^{-1} H_1 \\ \mathcal{R}_{\mathbb{Y}}\left(\widetilde{G}\right) &= G = H_1 + H_2 \end{aligned} \tag{C-13}$$

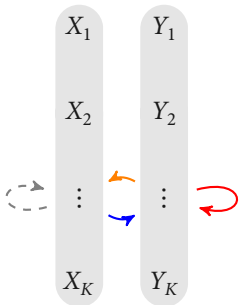

$$\cong \quad \widetilde{G} = \left(\begin{array}{c|c} O & I \\ \hline H_1 & H_2 \end{array}\right) \longmapsto \begin{cases} \mathcal{R}_{\mathbb{X}}(\widetilde{G}) & = (I - H_2)^{-1} H_1 \\ \mathcal{R}_{\mathbb{Y}}(\widetilde{G}) & = H_1 + H_2 \end{cases}$$

Figure 4: Embedding of G and its projection. Here, Ys are the orignal classes and X are their 'replicas'.

(Figure 4). On the other hand, we also have

$$(I - H_2)^{-1} H_1 = H_1 + H_2 (I - H_2)^{-1} H_1 = \mathcal{R}_{\mathbb{X}} \left(\begin{array}{c|c} H_1 & H_2 \\ \hline H_1 & H_2 \end{array}\right). \tag{C-14}$$

Since $H_1 (I - H_2)^{-1}$ and $H_2 (I - H_1)^{-1}$ have the same spectral radius, the following matrices share the same invasion conditions:

$$H_1 + H_2, \quad H_1 (I - H_2)^{-1}, \quad (I - H_2)^{-1} H_1 \quad \left(\begin{array}{c|c} H_1 & H_2 \\ \hline H_1 & H_2 \end{array}\right). \tag{C-15}$$

The relation to separation of timescales

We here show that the separation of timescales among classes produces the PNGM.

Theorem 4 (Constructing PNGM from continuous-time mutant dynamics)**.** Consider the following, K-dimensional mutant dynamics:

$$\frac{\mathrm{d}\overrightarrow{N'}}{\mathrm{d}t} = J\overrightarrow{N'}, \tag{C-16}$$

where $\overrightarrow{N'}$ represents a vector collecting the densities in the classes, and J represents the Jacobian, block-partitioned as Equation (C-1). Consider the Schur-complement $\mathcal{S}_{\mathbb{X}}(J) = J_{\mathbb{X},\mathbb{X}} - J_{\mathbb{X},\mathbb{Y}} J_{\mathbb{Y},\mathbb{Y}}^{-1} J_{\mathbb{Y},\mathbb{X}}$. Then,

(1) taking the quasi-equilibrium approximation $\mathrm{d}\overrightarrow{N'_{\mathbb{Y}}}/\,\mathrm{d}t \approx \overrightarrow{0}$ leads to $\mathrm{d}\overrightarrow{N'_{\mathbb{X}}}/\,\mathrm{d}t = \mathcal{S}_{\mathbb{X}}(J)\overrightarrow{N_{\mathbb{X}}}$;

(2) there exists a decomposition of $J = U - V$ that satisfies the hypotheses of NGM theorem, $V_{\mathbb{X},\mathbb{X}}$ nonsingular, and $\mathcal{S}_{\mathbb{X}}(J) = \mathcal{R}_{\mathbb{X}}\left(UV^{-1}\right)V_{\mathbb{X},\mathbb{X}} - V_{\mathbb{X},\mathbb{X}}$. Thus for such U, V with $UV^{-1} = G$, the resulting NGM is $\mathcal{R}_{\mathbb{X}}(G)V_{\mathbb{X},\mathbb{X}}\left(V_{\mathbb{X},\mathbb{X}}\right)^{-1} = \mathcal{R}_{\mathbb{X}}(G)$.

Proof. (1) This statement results from calculating the Schur-complement for the original K-dimensional Jacobian: consider the quasi-equilibrium approximation given by:

$$\frac{\mathrm{d}}{\mathrm{d}t}\overrightarrow{N'_{\mathbb{Y}}} = J_{\mathbb{Y},\mathbb{X}}\overrightarrow{N'_{\mathbb{X}}} + J_{\mathbb{Y},\mathbb{Y}}\overrightarrow{N'_{\mathbb{Y}}} \approx \overrightarrow{0}, \tag{C-17}$$

which gives $\overrightarrow{N'_{\mathbb{Y}}} \approx -J_{\mathbb{Y},\mathbb{Y}}^{-1} J_{\mathbb{Y},\mathbb{X}}\overrightarrow{N'_{\mathbb{X}}}$, and thus

$$\frac{\mathrm{d}\overrightarrow{N'_{\mathbb{X}}}}{\mathrm{d}t} \approx J_{\mathbb{X},\mathbb{X}}\overrightarrow{N'_{\mathbb{X}}} + J_{\mathbb{X},\mathbb{Y}}\overrightarrow{N'_{\mathbb{Y}}} \approx (J_{\mathbb{X},\mathbb{X}} - J_{\mathbb{X},\mathbb{Y}} J_{\mathbb{Y},\mathbb{Y}}^{-1} J_{\mathbb{Y},\mathbb{X}})\overrightarrow{N'_{\mathbb{X}}} = \mathcal{S}_{\mathbb{X}}(J)\overrightarrow{N'_{\mathbb{X}}}. \tag{C-18}$$

(2) It is easy to check that if we choose a block-diagonal, invertible, and inverse-nonnegative matrix as V, the theorem immediately follows. □

This theorem guarantees the equivalence of quasi-equilibrium approximation (sepataion of timescales) and PNGM: the primary group dynamics are taken as 'slow' while the secondary group dynamics are 'fast.'

We can consequently derive the discrete-time analogue of the separation of timescales.

Proposition 1 (Constructing PNGM from discrete-time mutant dynamics)**.** Suppose the mutant dynamics:

$$\overrightarrow{N'}(t+1) = G\overrightarrow{N'}(t), \tag{C-19}$$

where G represents a next-generation matrix of the system, block-partitioned as Equation (C-1). Then, the PNGM obtains by taking the quasi-equilibrium approximation of fast-primary group and slow-secondary group.

Proof. We explicitly solve $G_{\mathbb{Y},\mathbb{X}}\overrightarrow{N_{\mathbb{X}}} + G_{\mathbb{Y},\mathbb{Y}}\overrightarrow{N_{\mathbb{Y}}} \approx \overrightarrow{N_{\mathbb{Y}}}$ to get $\overrightarrow{N_{\mathbb{Y}}} \approx \left(I - G_{\mathbb{Y},\mathbb{Y}}\right)^{-1} G_{\mathbb{Y},\mathbb{X}}\overrightarrow{N_{\mathbb{X}}}$. Substituting this into the dynamics of $\overrightarrow{N_{\mathbb{X}}}$ yields

$$\overrightarrow{N_{\mathbb{X}}}(t+1) = G_{\mathbb{X},\mathbb{X}}\overrightarrow{N_{\mathbb{X}}} + G_{\mathbb{X},\mathbb{Y}}\overrightarrow{N_{\mathbb{Y}}} \approx \left(G_{\mathbb{X},\mathbb{X}} + G_{\mathbb{X},\mathbb{Y}}\left(I - G_{\mathbb{Y},\mathbb{Y}}\right)^{-1} G_{\mathbb{Y},\mathbb{X}}\right)\overrightarrow{N_{\mathbb{X}}} = \mathcal{R}_{\mathbb{X}}(G)\overrightarrow{N_{\mathbb{X}}}(t), \tag{C-20}$$

which proves the proposition. □

Reproductive values

Here we show that the eigenvectors for the primary group at neutrality are unchanged with the projection. Let $\vec{r}$ denote the right eigenvector of G° (at neutrality) associated with $\rho(G^\circ) = 1$:

$$G^\circ \vec{r} = \vec{r}. \tag{C-21}$$

Now suppose that the vector is partitioned so the dimension is consistent with the block-partitioning of G°; namely:

$$\begin{pmatrix}\overrightarrow{r_{\mathbb{X}}}\\ \overrightarrow{r_{\mathbb{Y}}}\end{pmatrix} = G^\circ\begin{pmatrix}\overrightarrow{r_{\mathbb{X}}}\\ \overrightarrow{r_{\mathbb{Y}}}\end{pmatrix} = \begin{pmatrix}G^\circ_{\mathbb{X},\mathbb{X}} & G^\circ_{\mathbb{X},\mathbb{Y}}\\ G^\circ_{\mathbb{Y},\mathbb{X}} & G^\circ_{\mathbb{Y},\mathbb{Y}}\end{pmatrix}\begin{pmatrix}\overrightarrow{r_{\mathbb{X}}}\\ \overrightarrow{r_{\mathbb{Y}}}\end{pmatrix} = \begin{pmatrix}G^\circ_{\mathbb{X},\mathbb{X}}\overrightarrow{r_{\mathbb{X}}} + G^\circ_{\mathbb{X},\mathbb{Y}}\overrightarrow{r_{\mathbb{Y}}}\\ G^\circ_{\mathbb{Y},\mathbb{X}}\overrightarrow{r_{\mathbb{X}}} + G^\circ_{\mathbb{Y},\mathbb{Y}}\overrightarrow{r_{\mathbb{Y}}}\end{pmatrix}. \tag{C-22}$$

By solving for $\overrightarrow{r_{\mathbb{Y}}}$ the linear equation at the second block, we have:

$$\overrightarrow{r_{\mathbb{Y}}} = \left(I - G^\circ_{\mathbb{Y},\mathbb{Y}}\right)^{-1} G^\circ_{\mathbb{Y},\mathbb{X}}\overrightarrow{r_{\mathbb{X}}}, \tag{C-23}$$

substituting which into the first block gives:

$$\overrightarrow{r_{\mathbb{X}}} = \left(G^\circ_{\mathbb{X},\mathbb{X}} + G^\circ_{\mathbb{X},\mathbb{Y}}\left(I - G^\circ_{\mathbb{Y},\mathbb{Y}}\right)^{-1} G^\circ_{\mathbb{Y},\mathbb{X}}\right)\overrightarrow{r_{\mathbb{X}}} = \mathcal{R}_{\mathbb{X}}(G^\circ)\overrightarrow{r_{\mathbb{X}}}, \tag{C-24}$$

as desired. The same argument applies to the left eigenvector associated with the spectral radius $\rho(G^\circ) = 1$.

D Stability analysis

We have presented various invadability-equivalent NGMs with $\kappa_1(\delta, z) \coloneqq \rho(G_1) - 1 \gtreqless 0$ if and only if $\kappa_2(\delta, z) \coloneqq \rho(G_2) - 1 \gtreqless 0$. From this expression, we can derive three properties of long-term evolutionary dynamics, namely (i) the location of evolutionary equilibrium (EE), (ii) convergence stability, and (iii) evolutionary stability.

We write sign() for the sign function.

Location of evolutionary equilibrium and convergence stability

We expand $\kappa_i(\delta, z)$ to the first order in δ as:

$$\kappa_i(\delta, z) = \delta\kappa_i^{(1)}(z) + O(\delta^2), \tag{D-1}$$

where $\kappa_i^{(1)}(z) := \left.\frac{\partial \kappa_i}{\partial \delta}\right|_{\delta=0}$ is the selection gradient, and the zero-th order term vanishes due to neutrality ($\kappa_i(0,z)=0$).

For any given resident trait z, $\kappa_1(\delta,z)$ and $\kappa_2(\delta,z)$ share the same sign for sufficiently small $|\delta|>0$. For this point-wise property to hold, their leading-order coefficients in the Taylor expansion evaluated at z must also share the same sign. Thus, we have:

$$\operatorname{sign}\left(\kappa_1^{(1)}(z)\right) = \operatorname{sign}\left(\kappa_2^{(1)}(z)\right). \tag{D-2}$$

From this equivalence, two properties immediately follow: (i) $\kappa_1^{(1)}(z^*)=0$ if and only if $\kappa_2^{(1)}(z^*)=0$, which proves that the location of the evolutionary equilibrium (EE) is identical. (ii) In the neighborhood of the EE, the sign of the selection gradient is identical for both measures. This implies that the direction of trait substitution is exactly the same, thereby ensuring that their convergence stability agrees.

Evolutionary stability

Fix the resident trait at an evolutionary equilibrium, $z=z^*$. We expand the fitness functions with respect to δ up to the second order:

$$\kappa_i(\delta,z^*) = \kappa_i(0,z^*) + \delta\kappa_i^{(1)}(z^*) + \frac{1}{2}\delta^2\kappa_i^{(2)}(z^*) + O\left(\delta^3\right). \tag{D-3}$$

The zero-th order term vanishes due to neutrality ($\kappa_i(0,z^*)=0$), and the first-order term vanishes because z^* is an evolutionary equilibrium ($\kappa_i^{(1)}(z^*)=0$).

Because $\kappa_1(\delta,z^*)$ and $\kappa_2(\delta,z^*)$ share the same sign for any sufficiently small $|\delta|>0$, their leading non-zero terms in the expansion must also share the same sign. Thus, we conclude that

$$\operatorname{sign}\left(\kappa_1^{(2)}(z^*)\right) = \operatorname{sign}\left(\kappa_2^{(2)}(z^*)\right), \tag{D-4}$$

which ensures that the condition for evolutionary stability is identical between any two invadability-equivalent NGMs.

Reproductive value-weighted selection gradient

We show that the selection gradients derived either by the original NGM and PNGM agree. Let us derive the selection gradient using the reproductive values: we write $\vec{\ell}^{\top}$ or $\vec{r}$ for the left or right eigenvector of neutral NGM G° associated with the spectral radius 1, respectively (Taylor & Frank 1996; Frank 1998; Avila & Mullon 2023). Given PNGM, we partition the eigenvectors according to the same partition-size:

$$\begin{aligned} \vec{\ell} &= \begin{pmatrix} \vec{\ell_{\mathbb{X}}} \\ \vec{\ell_{\mathbb{Y}}} \end{pmatrix}, \\ \vec{r} &= \begin{pmatrix} \vec{r_{\mathbb{X}}} \\ \vec{r_{\mathbb{Y}}} \end{pmatrix}. \end{aligned} \tag{D-5}$$

The first derivative of the PNGM, with the following lines being evaluated at neutrality $z'=z$ unless otherwise stated, is given by:

$$\begin{aligned} \frac{\partial \mathcal{P}(G(z',z))}{\partial \delta} &= \frac{\partial}{\partial \delta}\left(G_{\mathbb{X},\mathbb{X}} + G_{\mathbb{X},\mathbb{Y}}\left(I - G_{\mathbb{Y},\mathbb{Y}}\right)^{-1} G_{\mathbb{Y},\mathbb{X}}\right) \\ &= G^{(1)}_{\mathbb{X},\mathbb{X}} + G^{(1)}_{\mathbb{X},\mathbb{Y}}\left(I - G^\circ_{\mathbb{Y},\mathbb{Y}}\right)^{-1} G^\circ_{\mathbb{Y},\mathbb{X}} \\ &+ G^\circ_{\mathbb{X},\mathbb{Y}}\left(I - G^\circ_{\mathbb{Y},\mathbb{Y}}\right)^{-1} G^{(1)}_{\mathbb{Y},\mathbb{Y}}\left(I - G^\circ_{\mathbb{Y},\mathbb{Y}}\right)^{-1} G^\circ_{\mathbb{Y},\mathbb{X}} + G^\circ_{\mathbb{X},\mathbb{Y}}\left(I - G^\circ_{\mathbb{Y},\mathbb{Y}}\right)^{-1} G^{(1)}_{\mathbb{Y},\mathbb{X}}. \end{aligned} \tag{D-6}$$

Premultiplying the vector $\overrightarrow{\ell_{\mathbb{X}}^{\mathsf{T}}}$ and also postmultiplying $\overrightarrow{r_{\mathbb{X}}}$ gives:

$$\overrightarrow{\ell_{\mathbb{X}}^{\mathsf{T}}}\frac{\partial\mathcal{P}(G(z',z))}{\partial\delta}\overrightarrow{r_{\mathbb{X}}} = (\overrightarrow{\ell_{\mathbb{X}}^{\mathsf{T}}}, \overrightarrow{\ell_{\mathbb{Y}}^{\mathsf{T}}})\frac{\partial G(z',z)}{\partial\delta}\begin{pmatrix}\overrightarrow{r_{\mathbb{X}}}\\ \overrightarrow{r_{\mathbb{Y}}}\end{pmatrix} = \frac{\partial\rho(G)}{\partial\delta}, \tag{D-7}$$

because:

$$\left(I - G^{\circ}_{\mathbb{Y},\mathbb{Y}}\right)^{-1} G^{\circ}_{\mathbb{Y},\mathbb{X}}\overrightarrow{r_{\mathbb{X}}} = \overrightarrow{r_{\mathbb{Y}}}, \tag{D-8}$$

$$\overrightarrow{\ell_{\mathbb{X}}^{\mathsf{T}}}G^{\circ}_{\mathbb{X},\mathbb{Y}}\left(I - G^{\circ}_{\mathbb{Y},\mathbb{Y}}\right)^{-1} = \overrightarrow{\ell_{\mathbb{Y}}^{\mathsf{T}}}. \tag{D-9}$$

We have therefore confirmed the equivalence between the convergence stability conditions for the original and projected next-generation matrix.

E Analyses of the examples

Example 1: Two-class model

We describe the result of NGM by taking the decomposition of J to be:

$$U = \begin{pmatrix} b_1' - a_1' & b_2' \\ a_1' & 0 \end{pmatrix}, \quad V = \begin{pmatrix} m_1 & 0 \\ 0 & m_2 \end{pmatrix}. \tag{E-1}$$

We write $f_1 \coloneqq b_1'/(m_1 + a_1')$, $s \coloneqq a_1'/(m_1 + a_1')$ and $f_2 \coloneqq b_2'/(m_2)$ for the fecundity of class-1 individual, survival probability ($0 \le s \le 1$), and fecundity of class-2 individual, respectively. A direct calculation then gives:

$$G = UV^{-1} = \begin{pmatrix} b_1' - a_1' & b_2' \\ a_1' & 0 \end{pmatrix}\begin{pmatrix} {m_1}^{-1} & 0 \\ 0 & {m_2}^{-1} \end{pmatrix} = \begin{pmatrix} \frac{f_1 - s}{1 - s} & f_2 \\ \frac{s}{1 - s} & 0 \end{pmatrix}. \tag{E-2}$$

Using the invasion determinant yields the invasion condition, of:

$$-\det(I - G) = -\frac{1 - f_1 - sf_2}{1 - s} > 0. \tag{E-3}$$

We thus get the invasion condition in the main text. Note that we have not assumed anything about the sign of $f_1 - s$, and thus G need not be nonnegative.

Example 2: Epidemiological model

The mutant dynamics is given by:

$$\begin{aligned}
\frac{\mathrm{d}S_{\mathrm{f}}'}{\mathrm{d}t} &= \theta_{\mathrm{ff}}b_{\mathrm{f}}' \cdot \frac{S_{\mathrm{m}}^{\circ} + I_{\mathrm{m}}^{\circ}}{N_{\mathrm{T}}^{\circ}} \cdot (S_{\mathrm{f}}' + (1-\nu)I_{\mathrm{f}}') + \theta_{\mathrm{fm}}b_{\mathrm{m}}' \cdot \frac{S_{\mathrm{m}}' + I_{\mathrm{m}}'}{N_{\mathrm{T}}^{\circ}} \cdot (S_{\mathrm{f}}^{\circ} + (1-\nu)I_{\mathrm{f}}^{\circ}) + \gamma_{\mathrm{f}}'I_{\mathrm{f}}' - hS_{\mathrm{f}}' - \mu S_{\mathrm{f}}' \\
\frac{\mathrm{d}I_{\mathrm{f}}'}{\mathrm{d}t} &= \theta_{\mathrm{ff}}b_{\mathrm{f}}' \cdot \frac{S_{\mathrm{m}}^{\circ} + I_{\mathrm{m}}^{\circ}}{N_{\mathrm{T}}^{\circ}} \cdot \nu I_{\mathrm{f}}' + \theta_{\mathrm{fm}}b_{\mathrm{m}}' \cdot \frac{S_{\mathrm{m}}' + I_{\mathrm{m}}'}{N_{\mathrm{T}}^{\circ}} \cdot \nu I_{\mathrm{f}}^{\circ} + hS_{\mathrm{f}}' - \left(\mu + \gamma_{\mathrm{f}}' + \alpha_{\mathrm{f}}\right)I_{\mathrm{f}}' \\
\frac{\mathrm{d}S_{\mathrm{m}}'}{\mathrm{d}t} &= \theta_{\mathrm{mf}}b_{\mathrm{f}}' \cdot \frac{S_{\mathrm{m}}^{\circ} + I_{\mathrm{m}}^{\circ}}{N_{\mathrm{T}}^{\circ}} \cdot (S_{\mathrm{f}}' + (1-\nu)I_{\mathrm{f}}') + \theta_{\mathrm{mm}}b_{\mathrm{m}}' \cdot \frac{S_{\mathrm{m}}' + I_{\mathrm{m}}'}{N_{\mathrm{T}}} \cdot (S_{\mathrm{f}}^{\circ} + (1-\nu)I_{\mathrm{f}}^{\circ}) + \gamma_{\mathrm{m}}'I_{\mathrm{m}}' - hS_{\mathrm{m}}' - \mu S_{\mathrm{m}}' \\
\frac{\mathrm{d}I_{\mathrm{m}}'}{\mathrm{d}t} &= \theta_{\mathrm{mf}}b_{\mathrm{f}}' \cdot \frac{S_{\mathrm{m}}^{\circ} + I_{\mathrm{m}}^{\circ}}{N_{\mathrm{T}}^{\circ}} \cdot \nu I_{\mathrm{f}}' + \theta_{\mathrm{mm}}b_{\mathrm{m}}' \cdot \frac{S_{\mathrm{m}}' + I_{\mathrm{m}}'}{N_{\mathrm{T}}^{\circ}} \cdot \nu I_{\mathrm{f}}^{\circ} + hS_{\mathrm{m}}' - (\mu + \gamma_{\mathrm{m}}' + \alpha_{\mathrm{m}})I_{\mathrm{m}}'.
\end{aligned} \tag{E-4}$$

The resulting Jacobian reads:

$$J = \left(\begin{array}{c:c} U_{\mathrm{ff}} & U_{\mathrm{fm}} \\ \hdashline U_{\mathrm{mf}} & U_{\mathrm{mm}} \end{array}\right) - \left(\begin{array}{c:c} V_{\mathrm{f}} & O \\ \hdashline O & V_{\mathrm{mm}} \end{array}\right), \quad G = \left(\begin{array}{c:c} U_{\mathrm{ff}} & U_{\mathrm{fm}} \\ \hdashline U_{\mathrm{mf}} & U_{\mathrm{mm}} \end{array}\right)\left(\begin{array}{c:c} V_{\mathrm{f}}^{-1} & O \\ \hdashline O & V_{\mathrm{mm}}^{-1} \end{array}\right), \tag{E-5}$$

where, writing $x_{\mathrm{m}}^{\circ} \coloneqq (S_{\mathrm{m}}^{\circ} + I_{\mathrm{m}}^{\circ})/(N_{\mathrm{T}}^{\circ})$ for the sex ratio, $y_{\mathrm{f}}^{\circ} \coloneqq I_{\mathrm{f}}/N_{\mathrm{T}}$ for the proportion of infected females, and $\theta_{k,m}$ for the probability that an individual of sex k derives a gene from a parent of sex m (for diploid organisms, these are all 1/2):

$$\begin{aligned}
U_{\mathrm{ff}} &= \theta_{\mathrm{ff}} \begin{pmatrix} \eta_{\mathrm{f}}' x_{\mathrm{m}}^{\circ} & \eta_{\mathrm{f}}'(1-\nu) x_{\mathrm{m}}^{\circ} \\ 0 & \eta_{\mathrm{f}}' \nu x_{\mathrm{m}}^{\circ} \end{pmatrix}, \\
U_{\mathrm{fm}} &= \theta_{\mathrm{fm}} \begin{pmatrix} ,\eta_{\mathrm{m}}'(1 - x_{\mathrm{m}}^{\circ} - \nu y_{\mathrm{f}}^{\circ}) & \eta_{\mathrm{m}}'(1 - x_{\mathrm{m}}^{\circ} - \nu y_{\mathrm{f}}^{\circ}) \\ \eta_{\mathrm{m}}' \nu y_{\mathrm{f}}^{\circ} & \eta_{\mathrm{m}}' \nu y_{\mathrm{f}}^{\circ} \end{pmatrix}, \\
U_{\mathrm{mf}} &= \theta_{\mathrm{mf}} \begin{pmatrix} \eta_{\mathrm{f}}' x_{\mathrm{m}}^{\circ} & \eta_{\mathrm{f}}'(1-\nu) x_{\mathrm{m}}^{\circ} \\ 0 & \eta_{\mathrm{f}}' \nu x_{\mathrm{m}}^{\circ} \end{pmatrix}, \\
U_{\mathrm{mm}} &= \theta_{\mathrm{mm}} \begin{pmatrix} \eta_{\mathrm{m}}'(1 - x_{\mathrm{m}}^{\circ} - \nu y_{\mathrm{f}}^{\circ}) & \eta_{\mathrm{m}}'(1 - x_{\mathrm{m}}^{\circ} - \nu y_{\mathrm{f}}^{\circ}) \\ \eta_{\mathrm{m}}' \nu y_{\mathrm{f}}^{\circ} & \eta_{\mathrm{m}}' \nu y_{\mathrm{f}}^{\circ} \end{pmatrix}, \\
V_{\mathrm{f}} &= \begin{pmatrix} h + \mu & -\gamma_{\mathrm{f}}' \\ -h & \mu + \gamma_{\mathrm{f}}' + \alpha_{\mathrm{f}} \end{pmatrix}, \\
V_{\mathrm{m}} &= \begin{pmatrix} h + \mu & -\gamma_{\mathrm{m}}' \\ -h & \mu + \gamma_{\mathrm{m}}' + \alpha_{\mathrm{m}} \end{pmatrix}.
\end{aligned} \tag{E-6}$$

Although we can write down the Jacobian (which is four-by-four) as above, we here analyze the model more formally without doing so. This approach would help us more easily code numerical analyses. For this aim, we use tensor decomposition. Note that the idea underlying the tensor decomposition is symmetry; for example, the vertical transmission (from mother) to her offspring is independent of offspring sex (at random with no bias). This enables us to handle the four-by-four matrix in more compact, two-by-two form:

$$J = \left(\underbrace{\begin{pmatrix} \theta_{\mathrm{ff}} & \theta_{\mathrm{fm}} \\ \theta_{\mathrm{mf}} & \theta_{\mathrm{mm}} \end{pmatrix}}_{=\Theta} \otimes \begin{pmatrix} 1 & 0 \\ 0 & 1 \end{pmatrix}\right)\left(\eta_{\mathrm{f}}' \underbrace{\begin{pmatrix} 1 & 0 \\ 0 & 0 \end{pmatrix}}_{=\Pi_{\mathrm{f}}} \otimes \underbrace{\begin{pmatrix} x_{\mathrm{m}}^{\circ} & (1-\nu)x_{\mathrm{m}}^{\circ} \\ 0 & \nu x_{\mathrm{m}}^{\circ} \end{pmatrix}}_{=X_{\mathrm{m}}^{\circ}} + \eta_{\mathrm{m}}' \underbrace{\begin{pmatrix} 0 & 0 \\ 0 & 1 \end{pmatrix}}_{=\Pi_{\mathrm{m}}} \otimes \underbrace{\begin{pmatrix} 1-x_{\mathrm{m}}^{\circ}-\nu y_{\mathrm{f}}^{\circ} & 1-x_{\mathrm{m}}^{\circ}-\nu y_{\mathrm{f}}^{\circ} \\ \nu y_{\mathrm{f}}^{\circ} & \nu y_{\mathrm{f}}^{\circ} \end{pmatrix}}_{=X_{\mathrm{f}}^{\circ}}\right) - \begin{pmatrix} V_{\mathrm{f}} & O \\ O & V_{\mathrm{m}} \end{pmatrix}, \tag{E-7}$$

which, using the mixed-product rule (Graham 2018), we can rewrite as:

$$J = \left(\eta_{\mathrm{f}}' \Theta \Pi_{\mathrm{f}}\right) \otimes X_{\mathrm{m}}^{\circ} + \left(\eta_{\mathrm{m}}' \Theta \Pi_{\mathrm{m}}\right) \otimes X_{\mathrm{f}}^{\circ} - \begin{pmatrix} V_{\mathrm{f}} & O \\ O & V_{\mathrm{m}} \end{pmatrix}, \tag{E-8}$$

where Πs are projections:

$$\Pi_{\mathrm{f}} = \left(\begin{array}{c:c} I & O \\ \hdashline O & O \end{array}\right), \quad \Pi_{\mathrm{m}} = \left(\begin{array}{c:c} O & O \\ \hdashline O & I \end{array}\right). \tag{E-9}$$

We invert the last V-matrix and get NGM:

$$G = \left(\left(\eta_{\mathrm{f}}' \Theta \Pi_{\mathrm{f}}\right) \otimes \left(X_{\mathrm{m}}^{\circ}\right)\right) \begin{pmatrix} V_{\mathrm{f}} & O \\ O & V_{\mathrm{m}} \end{pmatrix}^{-1} + \left(\left(\eta_{\mathrm{m}}' \Theta \Pi_{\mathrm{m}}\right) \otimes \left(X_{\mathrm{f}}^{\circ}\right)\right) \begin{pmatrix} V_{\mathrm{f}} & O \\ O & V_{\mathrm{m}} \end{pmatrix}^{-1}. \tag{E-10}$$

Using Π_{f} and Π_{m}, we can rewrite the inversion as:

$$\begin{pmatrix} V_{\mathrm{f}} & O \\ O & V_{\mathrm{m}} \end{pmatrix}^{-1} = \begin{pmatrix} V_{\mathrm{f}}^{-1} & O \\ O & V_{\mathrm{m}}^{-1} \end{pmatrix} = \Pi_{\mathrm{f}} \otimes V_{\mathrm{f}}^{-1} + \Pi_{\mathrm{m}} \otimes V_{\mathrm{m}}^{-1}. \tag{E-11}$$

Again using the mixed product rule and $\Pi_{\mathrm{f}}\Pi_{\mathrm{m}} = O, \Pi_{\mathrm{f}}^2 = \Pi_{\mathrm{f}}$ and $\Pi_{\mathrm{m}}^2 = \Pi_{\mathrm{m}}$, we get:

$$G = \left(\eta_{\mathrm{f}}'\Theta\Pi_{\mathrm{f}}\right) \otimes \left(X_{\mathrm{m}}^{\circ} V_{\mathrm{f}}^{-1}\right) + \left(\eta_{\mathrm{m}}'\Theta\Pi_{\mathrm{m}}\right) \otimes \left(X_{\mathrm{f}}^{\circ} V_{\mathrm{m}}^{-1}\right). \tag{E-12}$$

We note that

$$V_{\mathrm{f}}^{-1} = \frac{1}{1-\iota\nu_{\mathrm{f}}'}\begin{pmatrix} \frac{1}{h+\mu} & \nu_{\mathrm{f}}' \\ \iota & \frac{1}{\mu+\gamma_{\mathrm{f}}'+\alpha_{\mathrm{f}}} \end{pmatrix}, \tag{E-13}$$

$$V_{\mathrm{m}}^{-1} = \frac{1}{1-\iota\nu_{\mathrm{m}}'}\begin{pmatrix} \frac{1}{h+\mu} & \nu_{\mathrm{m}}' \\ \iota & \frac{1}{\mu+\gamma_{\mathrm{m}}'+\alpha_{\mathrm{m}}} \end{pmatrix} \tag{E-14}$$

with $\iota = h/(h+\mu)$, $\nu_{\mathrm{f}}' = \gamma_{\mathrm{f}}'/(\mu+\gamma_{\mathrm{f}}'+\alpha_{\mathrm{f}})$ and $\nu_{\mathrm{m}}' = \gamma_{\mathrm{m}}'/(\mu+\gamma_{\mathrm{m}}'+\alpha_{\mathrm{m}})$. Taken together,

$$G = \left(\begin{array}{c:c} \theta_{\mathrm{ff}}G_{\mathrm{f}} & \theta_{\mathrm{fm}}G_{\mathrm{m}} \\ \hdashline \theta_{\mathrm{mf}}G_{\mathrm{f}} & \theta_{\mathrm{mm}}G_{\mathrm{m}} \end{array}\right). \tag{E-15}$$

For diploidy,

$$G = \frac{1}{2}\left(\begin{array}{c:c} G_{\mathrm{f}} & G_{\mathrm{m}} \\ \hdashline G_{\mathrm{f}} & G_{\mathrm{m}} \end{array}\right). \tag{E-16}$$

Since this takes the form of block-partitioned matrix in Box 1, the invasion condition reduces to:

$$\rho\left(\frac{G_{\mathrm{f}}+G_{\mathrm{m}}}{2}\right) > 1. \tag{E-17}$$

For haplodiploidy,

$$G = \left(\begin{array}{c:c} \frac{1}{2}G_{\mathrm{f}} & \frac{1}{2}G_{\mathrm{m}} \\ \hdashline G_{\mathrm{f}} & O \end{array}\right). \tag{E-18}$$

By applying the PNGM to eliminate the male class, we get:

$$\mathcal{P}_{\mathrm{f}}(G) = \frac{1}{2}G_{\mathrm{f}} + \frac{1}{2}G_{\mathrm{m}}G_{\mathrm{f}}. \tag{E-19}$$

The first component represents the direct transmission of genes from female to female, and the second component represents the indirect transmission from female to female via male. The invasion condition for haplodiploidy is thus

$$\rho\left(\frac{1}{2}G_{\mathrm{f}} + \frac{1}{2}G_{\mathrm{m}}G_{\mathrm{f}}\right) > 1. \tag{E-20}$$

Example 3: Lefkovitch model

We consider the following NGM:

$$G = \begin{pmatrix} g_{1,1} & g_{1,2} & g_{1,3} & g_{1,4} \\ g_{2,1} & g_{2,2} & 0 & 0 \\ 0 & g_{3,2} & g_{3,3} & 0 \\ 0 & 0 & g_{4,3} & g_{4,4} \end{pmatrix}. \tag{E-21}$$

This NGM does not have a closed form of spectral radius. We partition the classes into primary and secondary groups: $\mathbb{X} = \{1, 2, 3\}$ and $\mathbb{Y} = \{4\}$. The PNGM then reads:

$$\mathcal{P}_{\mathbb{X}}(G) = \begin{pmatrix} g_{1,1} & g_{1,2} & g_{1,3} \\ g_{2,1} & g_{2,2} & 0 \\ 0 & g_{3,2} & g_{3,3} \end{pmatrix} + \begin{pmatrix} g_{1,4} \\ 0 \\ 0 \end{pmatrix} \frac{1}{1 - g_{4,4}} \begin{pmatrix} 0 & 0 & g_{4,3} \end{pmatrix}. \tag{E-22}$$

The second matrix is zero except for the $(1, 3)$-rd element $g_{1,4}(1 - g_{4,4})^{-1} g_{4,3}$, which recovers the result of the main text.

To derive the 'canonical form' invasion condition $\sum_k f_k \prod_m s_m > 1$, we first partition the NGM into fecundity and transition components $G = F + S$, with:

$$F = \begin{pmatrix} f_{1,1} & f_{1,2} & f_{1,3} & f_{1,4} \\ 0 & 0 & 0 & 0 \\ 0 & 0 & 0 & 0 \\ 0 & 0 & 0 & 0 \end{pmatrix}, \quad S = \begin{pmatrix} s_{1,1} & 0 & 0 & 0 \\ s_{2,1} & s_{2,2} & 0 & 0 \\ 0 & s_{3,2} & s_{3,3} & 0 \\ 0 & 0 & s_{4,3} & s_{4,4} \end{pmatrix}. \tag{E-23}$$

Inverting $I - S$ yields:

$$(I - S)^{-1}_{m,k} = \frac{1}{1 - s_{k,k}} \prod_{i=k+1}^{m} \frac{s_{i,i-1}}{1 - s_{i,i}}, \quad m \geq k. \tag{E-24}$$

Since F has elements only in the first row, what we actually need is

$$(I - S)^{-1}_{m,1} = \frac{1}{1 - s_{1,1}} \prod_{i=2}^{m} \frac{s_{i,i-1}}{1 - s_{i,i}}. \tag{E-25}$$

Using this we get:

$$G = F\,(I - S)^{-1} = \begin{pmatrix} g_{1,1} & * & * & * \\ 0 & 0 & 0 & 0 \\ 0 & 0 & 0 & 0 \\ 0 & 0 & 0 & 0 \end{pmatrix}, \quad g_{1,1} = \sum_{m=1}^{K} \frac{f_{1,m}}{1 - s_{m,m}} \prod_{i=1}^{m-1} \frac{s_{i+1,i}}{1 - s_{i,i}}, \tag{E-26}$$

which thus says that $\rho(G) = g_{1,1}$, leading to the canonical form given in the main text following the transformation:

$$\begin{aligned} f_m &:= \frac{f_{1,m}}{1 - s_{m,m}}, \\ s_i &:= \frac{s_{i+1,i}}{1 - s_{i,i}}, \end{aligned} \tag{E-27}$$

by abuse of notation.

We can derive the same canonical form by recursively applying $\mathcal{P}_{\{1,2,3\}}, \mathcal{P}_{\{1,2\}}, \mathcal{P}_{\{1\}}$:

$$\begin{aligned} G = \begin{pmatrix} f_{1,1} + s_{1,1} & f_{1,2} & f_{1,3} & f_{1,4} \\ s_{2,1} & s_{2,2} & 0 & 0 \\ 0 & s_{3,2} & s_{3,3} & 0 \\ 0 & 0 & s_{4,3} & s_{4,4} \end{pmatrix} &\overset{\mathcal{P}_{\{1,2,3\}}}{\longmapsto} \begin{pmatrix} f_{1,1} + s_{1,1} & f_{1,2} & f_{1,3} \\ s_{2,1} & s_{2,2} & 0 \\ 0 & s_{3,2} & s_{3,3} \end{pmatrix} + \frac{1}{1 - s_{4,4}} \begin{pmatrix} 0 & 0 & f_{1,4} s_{4,3} \\ 0 & 0 & 0 \\ 0 & 0 & 0 \end{pmatrix} \\ &\overset{\mathcal{P}_{\{1,2\}}}{\longmapsto} \dots \\ &\overset{\mathcal{P}_{\{1\}}}{\longmapsto} f_{1,1} + s_{1,1} + \sum_{m=2}^{K} \frac{f_{1,m}}{1 - s_{m,m}} \prod_{i=1}^{m-1} \frac{s_{i+1,i}}{1 - s_{i,i}}. \end{aligned} \tag{E-28}$$

Rearranging the last quantity > 1 yields the canonical form of invasion condition, with the abuse of notation $f_m := f_{1,m}/(1 - s_{m,m})$

and $s_i := s_{i+1,i}/(1 - s_{i,i})$.

Example 4: Dispersal in stable habitats

Moran process

The transition probabilities $S_{k,m}$ are given by Equation (25) (e.g., Mullon & Lehmann 2014). Based on these probabilities, we can describe the dynamics of the number of mutants per patch as:

$$\begin{aligned} q_1'(t+1) - q_1'(t) &= \phi_0' \sum_{k=1}^{K} k q_k'(t) + \mu_2' q_2'(t) - (\phi_1' + \mu_1')\, q_1'(t), \\ &\vdots \\ q_m'(t+1) - q_m'(t) &= \mu_{m+1}' q_{m+1}'(t) + \phi_{m-1}' q_{m-1}'(t) - (\phi_m' + \mu_m')\, q_m'(t), \\ &\vdots \\ q_K'(t+1) - q_K'(t) &= \phi_{K-1}' q_{K-1}'(t) - \mu_K' q_K'(t). \end{aligned} \tag{E-29}$$

We now perform the separation of timescales. We eliminate the state variables in descending order from q_K', q_{K-1}', to q_2'. First, setting the left-hand side of the last line to zero yields $q_K' \approx \phi_{K-1}' q_{K-1}'/\mu_K'$. Second, we consider

$$q_K'(t+1) + q_{K-1}'(t+1) - (q_K'(t) + q_{K-1}'(t)) = \phi_{K-2}' q_{K-2}' - \mu_{K-1}' q_{K-1}' \tag{E-30}$$

and set it to zero to obtain

$$q_{K-1}' \approx \frac{\phi_{K-2}'}{\mu_{K-1}'} q_{K-2}'. \tag{E-31}$$

By induction, we have

$$q_m' \approx \frac{\phi_{m-1}'}{\mu_m'} q_{m-1}', \tag{E-32}$$

and thus

$$q_m' \approx q_1' \prod_{k=1}^{m-1} \frac{\phi_k'}{\mu_{k+1}'}, \quad m = 1, \dots, K. \tag{E-33}$$

Substituting these expressions into the dynamics of class 1 leads to:

$$q_1'(t+1) - q_1'(t) \approx \phi_0' \left(\sum_{m=1}^{K} m \left(\prod_{k=1}^{m-1} \frac{\phi_k'}{\mu_{k+1}'} \right) \right) q_1'(t) - \mu_1' q_1'(t). \tag{E-34}$$

The invasion condition is determined by requiring the right-hand side to be positive, which gives

$$\sum_{m=1}^{K} m \prod_{k=1}^{m} \frac{\phi_{k-1}'}{\mu_k'} > 1, \tag{E-35}$$

as desired.

The Wright-Fisher model and the advantage of the structural approach

The standard approach to evolutionary invasion analysis in subdivided populations, particularly under the Wright-Fisher process with local density dependence, heavily relies on tracking the probability distribution of local patch states (i.e., the number of mutants in a patch). As brilliantly demonstrated by Mullon et al. (2016, 2018), one can evaluate the invasion condition by differentiating the lineage fitness. However, because the Wright-Fisher process yields a dense transition matrix, analytically solving the recursions for the perturbed mutant distributions or identical-by-descent (IBD) probabilities requires remarkable

mathematical effort and biological intuition. This complexity severely limits the generalizability of the traditional approach when the model incorporates additional class structures such as sex, age, or environmental heterogeneity.

Here, we demonstrate how our structural framework, specifically the synthesis of the projected next-generation matrix (PNGM) and the invasion determinant, effortlessly bypasses this high-dimensional hurdle.

We start by constructing the full $K \times K$ next-generation matrix G for a focal patch, where the state $k \in \{1, 2, \dots, K\}$ represents the number of mutants in the patch. We biologically decompose the NGM into two distinct pathways: local philopatric transitions S and global seeding of new patches F, such that

$$G = F + S. \tag{E-36}$$

The matrix S describes the local demography (e.g., binomial sampling in the Wright-Fisher process) where mutants stay in the focal patch. Importantly, $\rho(S) < 1$ because without global seeding, the local mutant lineage is doomed to ultimate extinction under the infinite-island assumption.

The matrix F describes the production of successful emigrants that colonize resident patches. In the infinite-island model, a dispersing mutant will almost surely land in a patch entirely occupied by residents, creating a new local lineage starting with exactly one mutant. This biological feature implies a rank-one structure for F:

$$F = \vec{e_1}\vec{f}^{\top}, \tag{E-37}$$

where $\vec{e_1} = (1, 0, \dots, 0)^{\top}$ is the unit vector representing the new state of exactly one mutant, and $\vec{f} = (f_1, f_2, \dots, f_K)^{\top}$ is the vector whose k-th element represents the expected number of successful global seedings produced by a patch currently containing k mutants.

Under the traditional method, evaluating the spectral radius $\rho(G) > 1$ directly is analytically prohibitive for a dense matrix. However, using the invasion determinant, the invasion condition is equivalent to $-\det(I - G) > 0$. Substituting the rank-one structure into the determinant and applying the matrix determinant lemma (the Sherman-Morrison formula), we obtain:

$$\det(I - G) = \det\Big(I - S - \vec{e_1}\vec{f}^{\top}\Big) = \det(I - S)\det\Big(1 - \vec{f}^{\top}(I - S)^{-1}\vec{e_1}\Big). \tag{E-38}$$

Since $\rho(S) < 1$, we have $\det(I - S) > 0$. Thus, the invasion condition collapses exactly to a single scalar inequality:

$$W \coloneqq \vec{f}^{\top}(I - S)^{-1}\vec{e_1} > 1. \tag{E-39}$$

This scalar W is precisely the 1×1 PNGM projected onto the state of a newly seeded patch (i.e., primary group $\mathbb{X} = \{1\}$), the so-called metapopulation fitness (Metz & Gyllenberg 2001; Ajar 2003; Massol et al. 2009; Mullon et al. 2016). We have entirely eliminated the need to explicitly track the $K \times K$ mutant frequency dynamics. The matrix $(I - S)^{-1}$ is the fundamental matrix, where the k-th entry of $\vec{\tau} \coloneqq (I - T)^{-1}\vec{e_1}$ simply represents the expected sojourn time in state k starting from a single founder.

The true power of this structural approach shines under weak selection (first-order effects). Instead of solving complex recursions for the perturbed mutant distributions $\partial q_k/\partial\delta$ as required in previous studies (Mullon et al. 2016, 2018), we can mechanically Taylor-expand the scalar fitness W. Let δ be the small phenotypic deviation of the mutant. We expand $S \approx S^{\circ} + \delta S^{(1)}$ and $\vec{f} \approx \vec{f}^{\circ} + \delta\vec{f}^{(1)}$. Using the standard matrix identity for the derivative of an inverse, $(I - S)^{-1} \approx (I - S^{\circ})^{-1} + \delta\,(I - S^{\circ})^{-1}\,S^{(1)}\,(I - S^{\circ})^{-1}$, the selection gradient emerges automatically:

$$\left.\frac{\partial W}{\partial\delta}\right|_{\delta=0} = \vec{f}^{\top(1)}\vec{\tau}^{\circ} + \vec{\ell}^{\top}S^{(1)}\vec{\tau}^{\circ}, \tag{E-40}$$

where $\vec{\tau}^{\circ} = (I - S^{\circ})^{-1}\vec{e_1}$ is the neutral sojourn time vector, and $\vec{\ell}^{\top} = \vec{f}^{\circ\top}(I - S^{\circ})^{-1}$ is proportional to $(1, 2, \dots, K)^{\top}$.

In this formulation, the term $\vec{\ell}^{\top}S^{(1)\circ}$ elegantly and automatically generates the inclusive fitness effects (kin selection). Under

neutrality, all individuals are selectively equivalent and thus have the exact same individual reproductive value. Consequently, the total reproductive value of a patch (which corresponds to the class state in our NGM) is strictly proportional to the number of mutants it contains, enforcing $\vec{\ell} \propto (1, 2, \dots, K)^{\mathsf{T}}$. Thus, calculating $\vec{\ell}^{\mathsf{T}} S^{(1)} \vec{f}^{\circ}$ algebraically reduces to evaluating the neutral moments $\sum k \left(\vec{f}^{\circ}\right)_k$ and $\sum k^2 \left(\vec{f}^{\circ}\right)_k$, which are fundamentally linked to standard, readily available identity-by-descent (IBD) probabilities or relatedness coefficients.

Under Wright-Fisher demography the local transition matrix is typically dense, so the convenient tri-diagonal recursions used above no longer apply; nevertheless, the metapopulation-fitness criterion still reduces to the scalar condition.

References

Ajar, É. (2003). Analysis of disruptive selection in subdivided populations. *BMC Evol. Biol.*, **3**.1, p. 22. DOI: 10.1186/1471-2148-3-22.

Avila, P. & Mullon, C. (2023). Evolutionary game theory and the adaptive dynamics approach: adaptation where individuals interact. *Phil. Trans. R. Soc. B*, **378**.1876. DOI: 10.1098/rstb.2021.0502.

Berman, A. & Plemmons, R. J. (1987). *Nonnegative matrices in the mathematical sciences*. Classics in applied mathematics 9. Society for Industrial and Applied Mathematics.

Crabtree, D. E. & Haynsworth, E. V. (1969). An identity for the Schur complement of a matrix. *Proc. Am. Math. Soc.*, **22**.2, pp. 364–366. DOI: 10.1090/s0002-9939-1969-0255573-1.

Frank, S. A. (1998). *Foundations of social evolution*. Princeton University Press.

Graham, A. (2018). *Kronecker products and matrix calculus with applications*. Courier Dover Publications.

Horn, R. A. & Johnson, C. R. (1985). *Matrix Analysis*. **169**. Cambridge University Press, Cambridge.

Massol, F., Calcagno, V., & Massol, J. (2009). The metapopulation fitness criterion: Proof and perspectives. *Theor. Popul. Biol.*, **75**.2–3, pp. 183–200. DOI: http://dx.doi.org/10.1016/j.tpb.2009.02.005.

Metz, J. A. & Gyllenberg, M. (2001). How should we define fitness in structured metapopulation models? Including an application to the calculation of evolutionarily stable dispersal strategies. *Proc. R. Soc. B*, **268**.1466, pp. 499–508.

Mullon, C., Keller, L., & Lehmann, L. (2016). Evolutionary stability of jointly evolving traits in subdivided populations. *Am. Nat.*, **188**.2, pp. 175–195. DOI: 10.1086/686900.

— (2018). Social polymorphism is favoured by the co-evolution of dispersal with social behaviour. *Nat. Ecol. Evol.*, **2**.1, p. 132. DOI: 10.1038/s41559-017-0397-y.

Mullon, C. & Lehmann, L. (2014). The robustness of the weak selection approximation for the evolution of altruism against strong selection. *J. Evol. Biol.*, **27**.10, pp. 2272–2282. DOI: 10.1111/jeb.12462.

Roberts, M. G. & Heesterbeek, J. A. P. (2003). A new method for estimating the effort required to control an infectious disease. *Proc. R. Soc. B*, **270**.1522, pp. 1359–1364. DOI: 10.1098/rspb.2003.2339.

Taylor, P. D. & Frank, S. A. (1996). How to make a kin selection model. *J. Theor. Biol.*, **180**.1, pp. 27–37. DOI: 10.1006/jtbi.1996.0075.

Varga, R. S. (1963). *Matrix iterative analysis*. Graduate Texts in Mathematics. Prentice–Hall, Englewood Cliffs, NJ.